1 **Nutrient and mercury deposition and storage in an alpine snowpack of the Sierra Nevada,**
2 **USA**

3 Christopher Pearson[1,2,3], Rina Schumer[1,3], Benjamin D. Trustman[2,3],

4 Karl Rittger[4], Dale W. Johnson[3,5], Daniel Obrist[2,3]

5 [1]Desert Research Institute, Division of Hydrologic Sciences, Reno, NV

6 [2]Desert Research Institute, Division of Atmospheric Sciences, Reno, NV

7 [3]University of Nevada-Reno, Graduate Program of Hydrologic Sciences, Reno, NV

8 [4]National Snow and Ice Data Center, Boulder, CO

9 [5]University of Nevada-Reno, Department of Natural Resources and Environmental Science,
10 Reno, NV

11

12

15

16

17

18

19

20

21

22

23

24

25

26

27 Corresponding author: Christopher C. Pearson, Desert Research Institute, 2215 Raggio Parkway,

28 Reno, Nevada 89512, E-mail: ChrisCPearson86@gmail.com

29   **Abstract**

30   Bi-weekly snowpack core samples were collected at seven sites along two elevation

31   gradients in the Tahoe Basin during two consecutive snow years to evaluate total wintertime

32   snowpack accumulation of nutrients and pollutants in a high elevation watershed of the Sierra

33   Nevada. Additional sampling of wet deposition and detailed snow pit profiles were conducted

34   the following year to compare wet deposition to snowpack storage and assess the vertical

35   dynamics of snowpack nitrogen, phosphorus, and mercury. Results show that on average organic

36   N comprised 48% of all snowpack N, while nitrate (NO_3^--N) and TAN (total ammonia nitrogen)

37   made up 25% and 27%, respectively. Snowpack NO_3^--N concentrations were relatively uniform

38   across sampling sites over the sampling seasons and showed little difference between seasonal

39   wet deposition and integrated snow pit concentrations. These patterns are in agreement with

40   previous studies that identify wet deposition as the dominant source of wintertime NO_3^--N

41   deposition. However, vertical snow pit profiles showed highly variable concentrations of NO_3^--N

42   within the snowpack indicative of additional deposition and in snowpack dynamics. Unlike NO_3^-

43   -N, snowpack TAN doubled towards the end of winter, which we attribute to a strong dry

44   deposition component which was particularly pronounced in late winter and spring. Organic N

45   concentrations in the snowpack were highly variable (from 35% to 70%) and showed no clear

46   temporal, spatial, or vertical trends throughout the season. Integrated snowpack organic N

47   concentrations were up to 2.5 times higher than seasonal wet deposition, likely due to microbial

48   immobilization of inorganic N as evident by coinciding increases of organic N and decreases of

49   inorganic N, in deeper, aged snow. Spatial and temporal deposition patterns of snowpack P were

50   consistent with particulate-bound dry deposition inputs and strong impacts from in-basin sources

51   causing up to 6 times enrichment at urban locations compared to remote sites. Snowpack Hg

52 showed little temporal variability and was dominated by particulate-bound forms (78% on

53 average). Dissolved Hg concentrations were consistently lower in snowpack than in wet

54 deposition which we attribute to photochemical-driven gaseous remission. In agreement with this

55 pattern is a significant positive relationship between snowpack Hg and elevation, attributed to a

56 combination of increased snow accumulation at higher elevations causing limited light

57 penetration and lower photochemical re-emission losses in deeper, higher elevation snowpack.

58 Finally, estimates of basin-wide loading based on spatially extrapolated concentrations and a

59 satellite-based snow water equivalent reconstruction model identify snowpack chemical loading

60 from atmospheric deposition as a substantial source of nutrients and pollutants to the Lake Tahoe

61 basin, accounting for 113 t of N, 9.3 t of P, and 1.2 kg of Hg each year.

1 Introduction

62

63   Atmospheric deposition accounts for significant nutrient and pollutant input to high

64 elevation watersheds such as the Sierra Nevada (Dolislager, 2006; Fain et al., 2011; McDaniel,

65 2013; Sickman et al., 2003; TERC, 2011; Vicars and Sickman, 2011; Williams and Melack,

66 1991a, b). Sierra Nevada snowpack supplies the majority of water to downstream communities

67 as well as to some of the nation's largest agricultural areas. Quantifying atmospheric deposition

68 in alpine watersheds is challenging because of large spatial variability in deposition rates caused

69 by complex terrain, precipitation gradients, and varied origins of atmospheric constituents (i.e.

70 local versus regional and global, natural versus anthropogenic; Jassby et al., 1994 ; Rohrbough et

71 al., 2003). Single-site measurements, therefore, do not allow for accurate extrapolation of

72 nutrient or pollutant deposition in alpine regions and broader temporal and spatial data is needed

73 to assess the mass and dynamics of atmospheric inputs.

74   In this study, we used multiple and repeated sampling of full depth snowpack cores

75 (integrated snowpack sampling) across the Lake Tahoe basin to quantify atmospheric deposition

76 loads and patterns from the first snowfall until the end of melting. Snowpack acts as an

77 integrating reservoir for water, solutes, and particulates that deposit throughout winter and spring

78 (Turk et al., 2001). Wet deposition, in the form of snowfall and rain, directly accumulates in the

79 developing snowpack throughout the snow season (Kuhn, 2001). Additionally, during storm-free

80 periods, snowpack also receives dry deposition which often is complicated to quantify since dry

81 deposition samplers can be biased due to different collection efficiencies compared to natural

82 surfaces (Jassby et al., 1994). Representing a natural surface that covers the ground for several

83 months of the year, snowpack sampling thereby can provide accurate on-the-ground

84 measurements of total (bulk: wet and dry) deposition occurring in mountainous areas.

85   While the snowpack integrates wintertime atmospheric deposition input, it also records

86 chemical and physical transformations that occur during storage such as elution during melt

87 events, chemical transformations, and volatilization. For example, ionic pulses of anions and

88 cations occur upon snowpack melt whereby ions are thought to be mobilized in the following

89 order: SO_4^{2-} >NO_3^- >Cl^- >alkali metals >alkaline earth metals >cations (other than NH_4^+) >anions

90 >NH_4^+ > H_2O_2 (Berg, 1992; Brooks and Williams, 1999; Kuhn, 2001; Stottlemyer and

91 Rutkowski, 1990; Williams and Melack, 1991b). In addition, pollutants such as Hg and

92 persistent organic pollutants (POPs) as well as nutrients can undergo photochemical

93 transformations and be subject to substantial gaseous re-emission to the atmosphere (Fain et al.,

94 2011; Halsall, 2004; Lalonde et al., 2002; Poulain et al., 2007). Specific examples include

95 photochemical reduction and remission of mercury (Hg) during snowpack storage as well as

96 photolysis and emission of nitrate (NO_3^-) from polar snow (Galbavy et al., 2007; Jacobi and

97 Hilker, 2007; Rothlisberger et al., 2002). In addition, microbial activity in and under the seasonal

98 snowpack can play an important role in snowpack N dynamics (Brooks et al., 1996; Williams et

99 al., 1996); even in Artic environments with low temperatures and minimal water content (Larose

100 et al., 2013). Therefore, snowpack sampling yields relevant temporal atmospheric deposition

101 patterns in conjunction with post-depositional chemical losses or conversions.

102   Spatially, snowpack sampling can be an elegant tool to quantify gradients in atmospheric

103 deposition that are difficult to assess with other methods; for example, the Sierra Nevada show

104 strong orographic precipitation effects, with the leeward side receiving significantly less

105 precipitation than the windward side (O'Hara et al., 2009). Such different precipitation patterns

106 can cause large differences in wet deposition across mountain ranges (Fain et al., 2011; NADP,

107 2012). Assessing spatial deposition patterns using snowpack sampling at multiple locations

108 across a watershed should allow for better characterization of basin-wide deposition patterns as

109 well as assessment of impacts of nearby urban areas versus regional and global sources of

110 atmospheric deposition (Brown et al., 2011; Kuhn, 2001; Morales-Baquero et al., 2006; Vicars

111 and Sickman, 2011).

112   The main goal of this study was to quantify N, P, and Hg concentrations and loads in

113 Sierra Nevada snowpack in order to characterize the magnitude, origin, and fate of atmospheric

114 deposition of nutrients and pollutants that accumulate throughout the winter and spring in this

115 mountain range. We quantified chemical loading at seven sites in the Lake Tahoe basin, along

116 two elevation transects, throughout the duration of two full snow seasons. Sampling included bi-

117 weekly snowpack cores (full profile; integrated snowpack samples) representing an integrated

118 load of constituents in the developing snowpack collected throughout the 2011-12 and 2012-13

119 snow years. In addition, volume-weighted wet deposition measured at two sites in 2013-14 was

120 compared to snowpack accumulation and detailed vertical snow pit profiles in that year to

121 compare snowpack accumulation to wet deposition and to further study in-snowpack chemical

122 dynamics. Finally, basin-wide loading estimates (mass area^{-1}) were calculated by spatially

123 extrapolating nutrient and pollutant measurements across the basin combined with a satellite-

124 based snowpack reconstruction model.

125 **2   Materials and Methods**

126 **2.1   Study Site**

127   The Lake Tahoe watershed lies in the northern portion of the Sierra Nevada range along

128 the border of Nevada and California. Renowned for its intense blue color and water clarity, this

129 lake has become a national landmark and tourism hotspot. Lake clarity measurements have

130   decreased, however, from approximately 30.5 m to 21.3 m since the 1960s due to eutrophication

131   from increased input of N and P, as well as additional input of light scattering particulates

132   (TERC, 2011). Directly west and upwind of the basin lies the central valley of California and

133   cities of Sacramento and San Francisco, California, which are suspected of contributing

134   significant amounts of nutrients and pollutants to the basin through agricultural and industrial

135   emissions.

136   Including all drainages, the Lake Tahoe watershed has an area of 1,310 km^2 (Figure 1).

137   The lake is 19 km wide and 35 km long with a total surface area of 495 km^2. The lake lies at

138   1,897 m above sea level and is on average 300 m deep. Surrounding the lake on all sides are

139   mountains up to elevations of 3,068 m. At the lake's surface, summer temperatures on average

140   reach 27^0 C and wintertime lows reach -9^0 C. Precipitation patterns in the watershed are highly

141   dependent on elevation with an average annual precipitation of 0.76 m at lake level and an

142   average of 2.03 m falling at higher elevations in the surrounding mountains (Fram, 2011).

143   Extreme snow events in this area are common and often produce snowpack depths greater than

144   4.5 m at high elevations. Rain shadow effects typically lead to decreased snow loading on the

145   downwind, eastern side of the basin. Approximately two-thirds of Lake Tahoe basin parent

146   material is granitic and one-third is volcanic (LTTMDL, 2008). Vegetation, consisting of mixed

147   coniferous forest and montane-subalpine species, cover approximately 80% of the basin

148   (LTTMDL, 2010). Areas of dense urban development occur along the shoreline at South Lake

149   Tahoe, Tahoe City, and Incline Village. Large portions of the northern and western shores are

150   occupied by seasonal cabins, while much of the eastern shore is undeveloped.

2.2 Sample Collection

2.2.1 Integrated snowpack sampling: 2011-12 and 2012-13 snow years

During the 2011-12 and 2012-13 water years, full snowpack bi-weekly core samples were collected at seven sites in the basin starting from the first measureable snowpack until the majority of spring melting occurred (2011-12: n= 49; 2012-13: n=56). This included mid-January through mid-April in 2012 and December to early-April in 2012-13. The seven sites were distributed along eastern and western elevation transects (Figure 1). Three of the sites were located at lake level (one remote site; two sites in urban areas; elevation approximately 1900 m); two sites were at mid-mountain elevation (approximately 2200 m); and two sites were at high elevation close to the mountain ridges (elevation approximately 2500 m). To minimize throughfall signals, we selected areas that were free of canopy coverage and had minimal snowpack disturbance (i.e., away from congested areas). Canopy effects on total snow accumulation are incorporated in the SWE reconstruction model. However, measurements of deposition and chemical snowpack storage are based on canopy-free, open locations, and do not include effects of forest cover.

Samples were collected using a Mt. Rose Federal Sampler and were immediately transferred to Whirl-pack© clean bags and a cooler with blue ice packs. Samples were transported within four hours to the Desert Research Institute in Reno, NV for storage at -20° C until laboratory analysis could be completed. Depth and snow water equivalent (SWE) were measured for each core using the Mt. Rose Federal Sampler. In cases of low snow accumulation, multiple cores were collected and homogenized to provide sufficient sample for all analyses. During collection, sterile gloves were worn, and soil contact and contamination were avoided in order to capture only constituents stored within the snowpack. While sampling, the first core

174   taken at each site was discarded in order to avoid carryover from previous sampling. Between

175   each sampling campaign, the Federal Sampler was cleaned with Milli-Q deionized water (<18.2

176   M Ω) and a chelating soap in accordance with trace metal sampling procedures (EPA, 2002).

177   Field blanks were measured by rinsing the sampler with Milli-Q water prior to each sampling

178   campaign.

179   **2.2.2   Wet deposition sampling and snow pit collection: 2013-14 snow year**

180   In order to differentiate between snowpack storage and wet deposition and further asses

181   dynamics in the snowpack, additional sampling of full snow pit profiles and wet deposition was

182   completed during the 2013-14 snow year. Bi-weekly wet deposition sample collection following

183   National Atmospheric Deposition Program protocol (http://nadp.sws.uiuc.edu/) was conducted at

184   the two high altitude sites by N-Con dual port trace metal samplers (Model TM 00-127; N-Con

185   Inc., Crawford, GA, USA). These samplers allowed for collection of real-time wet deposition

186   samples of both nutrients (N, P, and S) and Hg without cross contamination. The sample trains

187   consists of a NADP standard (19-128) glass funnel, a glass anti-evaporation capillary, a glass

188   sample bottle (2 liter) for collection of Hg, and a (19-130) polyethylene funnel with connector

189   and 1.5 liter HDPE sample container for nutrients. The glass sample bottle was pre-charged with

190   20 mL of deionized water and 0.5 mL of 12M HCl (EMD Omnitrace HX0607) to act as a

191   preservative for Hg. Sample bottles were collected in the field and kept in a cooler during

192   transport back to the Desert Research Institute in Reno, NV. Sample bottles were then weighed

193   in the lab and decanted into 250 mL HDPE bottles for nutrient samples and glass containers for

194   Hg samples. All samples were stored in refrigerators until processing.

195   Three snow pit analyses were conducted at the high elevation sites, two near the Mt. Rose

196   site (3/1/14 and 4/4/14) and one at the Homewood High site (2/28/14). The snow pit measured a

197 minimum of a 1.5 m^2 and was dug from the snow surface to the ground. Measuring sticks were

198 placed on either side of the pit face. A measurement of height, layer density, and crystal form

199 was noted. Snow samples were collected vertically every 10 cm using a 1000 cm^3 Kelly wedge

200 cutter (Model: RIP 1 Cutter; Snowmetrics, Fort Collins, CO, USA). Prior to collection, the acid

201 washed wedge was inserted into the snow adjacent to the sample wall two to three times at each

202 layer before sampling to avoid carry over. Duplicate samples were collected at each height and

203 analyzed separately. All samples were double bagged in Whirl-pack© clean bags and weighed

204 for density. Samples were then transferred to -20^0 C storage at the Desert Research Institute in

205 Reno, NV until analysis. Reported concentrations and densities are averages of the duplicate

206 samples.

2.3   Laboratory Analysis

208   Samples were analyzed for nitrite (NO_2^--N), nitrate (NO_3^--N), total ammonia nitrogen

209 (TAN; $NH_3 + NH_4^+$), total Kjeldhal nitrogen (TKN), orthophosphate (o-PO_4), total phosphorus

210 (TP), total Hg (THg, no filtration), and dissolved Hg (DHg, filtration). Prior to analysis, all

211 samples were removed from the freezer and placed in a dark cabinet at room temperature for

212 approximately 18 hours to melt. Once fully melted, the samples were thoroughly mixed and

213 dispensed into various aliquots for each analysis. Subsamples of NO_2^--N, NO_3^--N, TAN, SO_4^{2-},

214 and o-PO_4 were filtered through 0.45 μm filters (Pall Supor©) prior to analysis. Laboratory filter

215 blanks were approximately <2 ug L^{-1} for NO_2^--N, 6 ug L^{-1} for NO_3^--N, 5 ug L^{-1} for TAN, <20 ug

216 L^{-1} for SO_4^{2-}, and 2 ug L^{-1} for o-PO_4.

217   Ortho-phosphate and TP were measured according to EPA Standard Method (SM) 365.1

218 and SM 365.1/USGS I-4600-85, respectively (EPA, 1993; USGS, 1985). Method Detection

219 limits (MDL) for these techniques were 0.60 μg L^{-1} and 0.63 μg L^{-1}, respectively. Both

220   techniques employed colorimetric measurement with ascorbic acid. Prior to measurement of TP,

221   samples were digested with persulfate. Absorbance was then measured through flow injection

222   analysis (FIA; Rapid Flow Analyzer 300 equipped with an Astoria-Pacific 305D high sensitivity

223   photometer detector; Alpkem, College Station, TX).

224   Nitrite, NO_3^--N, and TAN analyses followed EPA SM 353.2 and SM 353.1 (EPA, 1979,

225   1993). Nitrite and NO_3^--N MDLs were 0.84 µg L^{-1}, and the TAN MDL was 0.77 µg L^{-1}. Nitrite

226   and NO_3^--N were measured by automated colorimetric analysis with cadmium reduction being

227   applied for the nitrate samples. Each sample was then measured by FIA (Rapid Flow Analyzer

228   300 equipped with an Astoria-Pacific 305D high sensitivity photometer detector; Alpkem,

229   College Station, TX). TAN samples were analyzed using automated phenate colorimetric

230   techniques. Total Kjeldhal Nitrogen was analyzed using automated phenate block digestion

231   according to EPA method 351.2. The MDL for TKN was 11.3 µg L^{-1}. Organic N (bulk) was

232   calculated as the difference between TKN and TAN. All nitrogen species were reported as

233   [ug L^{-1}]-N with total N calculated as the sum of organic N, TAN, and NO_3^--N. All snow sample

234   NO_2^- concentrations were below the DL.

235   Sulfate was determined using a chromatography system (ICS 2000 with Chromeleon

236   Software version 6.6 and AS14A Column; Dionex Inc., Sunnyville, CA) by EPA Method 300.0

237   (EPA, 1979). The MDL for SO_4^{2-} was 19 µg L^{-1}.

238   Total Hg and DHg were measured using a water analyzer (Model 2600; Tekran Inc.,

239   Toronto, Canada) according to EPA method 1631 revision E (EPA, 2002). For DHg samples,

240   approximately 50 mL of sample were filtered through a 0.45 µm filter (Acrodisc syringe filter

241   with Supor® Membrane; Pall Corporation, Port Washington, NY) while for THg, 50 mL of

242   sample were poured directly into a vial for analysis. Laboratory filter blanks were below the

243   detection limit (DL) of the system (<0.3 ng L^{-1}). Samples were preserved with 10% bromine

244   chloride (BrCl) solution for storage until analysis the next day. Before analysis, excess BrCl was

245   neutralized with pre-purified hydroxylamine hydrochloride. During analysis, samples were

246   automatically mixed with stannous chloride (SnCl$_2$) in a phase separator; reducing oxidized Hg

247   to elemental Hg. Elemental Hg is then loaded onto two sequential gold traps by an argon carrier

248   gas. The Hg is then released through thermal desorption and detected using atomic fluorescence

249   spectrometry. The Tekran Model 2600 was calibrated using a NIST SRM-3133 Hg standard

250   (with concentrations of 0, 0.5, 1.0, 5.0, 10.0, 25.0, and 50.0 ng L^{-1} Hg). System reliability was

251   checked using ongoing precision recovery injections of 5 ng L^{-1} throughout each run and ranged

252   between 87% to 112% recovery. Reagent blanks measured regularly throughout each run

253   ensured no contamination of the system. DLs calculated as three times the standard deviation of

254   the calibration blanks, averaged 0.3 ng L^{-1} for all runs. Particulate Hg was calculated as the

255   difference between THg and DHg.

256   **2.4   Statistics**

257   We performed analysis of variance (ANOVA) for all chemical species using the

258   following independent variables: (i) year (n=2, 2011-12 and 2012-13); (ii) site elevation (n=3;

259   low, mid- and high elevation site); (iii) location (n=2; eastern and western basin); and season

260   (n=2; early season [December through February] and late season [March and April]). ANOVAs

261   attribute variance of dependent variables to these various independent variables and test their

262   significance against the residual variance. All relationships were considered statistically

263   significant when p-values were ≤ 0.05.

264   Integrated snowpack concentrations were calculated by weighting each 10 cm snow pit

265   layer by its density. Seasonal wet deposition was calculated by weighting all wet deposition

266   samples by their volume up to the date of sampling. Linear regression analyses were performed

267   to test for correlations between snowpack chemical concentrations, SWE, and elevation. All

268   error bars in figures represent standard error.

269   **2.5   Basin-wide Modeling with SWE Reconstruction**

270   Basin-wide loads and distribution were assessed using chemical concentrations and loads

271   measured throughout the 2011-12 and 2012-13 snow seasons as well as basin-wide mean peak

272   SWE estimates from SWE reconstruction for the Sierra Nevada from 2000 to 2011 (Rittger,

273   2012). SWE reconstruction uses estimates of snow energy balance with areal snow cover

274   depletion from MODIS Snow Covered Area and Grain size (MODSCAG) (Rittger, 2011).

275   MODSCAG calculates fractional snow cover area and grain size from Moderate Resolution

276   Imaging Spectroradiometer (MODIS) data (Painter et al., 2009). Compared with previous

277   methods, MODSCAG has proven to give reliable depletion rates throughout the spring season

278   when snowmelt is highest (Rittger et al., 2013). Finally, the spatially refined MODSCAG data

279   set was combined with energy balance and temperature data to give accurate reconstructed

280   estimates of SWE throughout the Sierra Nevada, and specifically the Lake Tahoe Basin. At the

281   time of our study, SWE reconstruction data were only available for 2000 to 2011, with no

282   information from our sampling seasons, 2011-12 or 2012-13. The 2000 to 2011 data set includes

283   both high and low accumulation snow years and gives a reasonable representation of average

284   snowpack accumulation in the Lake Tahoe basin. In order to give an estimate of average annual

285   snowpack chemical storage, we applied the decadal average peak SWE for 2000 to 2011 to our

286   data (Figure 2a). Estimates made during this study were to establish relationships to previous

287   estimates of the Lake Tahoe nutrient budget and were not meant to represent a completely

288   accurate distribution or load stored within the basin's snowpack each year.

289   Snowpack sampling throughout the Lake Tahoe basin during 2011-12 and 2012-13

290   allowed for assessment of spatial and temporal chemical deposition patterns. Specifically,

291   relationships to wet or dry deposition, in-basin or out-of-basin sources, and early or late season

292   increases were identified. These deposition and source controls were then related to orographic

293   characteristics to estimate chemical concentrations throughout the basin in unknown areas. A

294   GIS land-use layer of the Tahoe Basin (LTTMDL, 2010) was applied in order to separate urban

295   and non-urban locations with similar orographic characteristics for urban influenced species (i.e.

296   TP). These scaled concentrations were then applied to SWE reconstruction estimates to

297   determine total snowpack chemical loading throughout the entire basin.

298   Snowpack sampling occurred in open areas free of canopy coverage, but it is possible

299   that tree and plant particulate matter still were incorporated in the snowpack. Litterfall

300   contributions represent a form of chemical recycling and will cause an overestimate of

301   atmospheric contributions made during this study. Visual inspection of snow samples, however,

302   showed low contributions of plant detritus in samples, and due to consistent forest types present

303   across the basin we would expect any additional plant-derived inputs to be random and unbiased

304   across sites.

305   **3   Results and Discussion**

306   **3.1   Spatial and temporal trends of snow accumulation and SWE**

307   In the Lake Tahoe basin, approximately 70% of annual precipitation falls during the

308   winter and spring as snow (Fram, 2011). The 2011-12, 2012-13, and 2013-14 winter seasons

309   were marked by relatively low snow accumulation. Peak basin average snowpack storage (April

310   1) for the central Sierra Nevada during 2011-12, 2012-13, and 2013-14 was approximately 50%,

311   53%, and 41% of the historical average (1951-present), respectively (CADWR, 2014). Although

312   peak SWE was similar in each season, the temporal trends in snow accumulation and spatial

313   distributions differed (Figure 3). In 2011-12, the Lake Tahoe Basin experienced low snowpack

314   accumulation until the middle of January, when a series of storms led to solid snow cover

315   throughout the basin. January storms were followed by a hiatus until late February and March

316   when a series of storms brought peak basin average SWE up to approximately 625 mm. The

317   2012-13 snow year started earlier, with late December storms bringing nearly 750 mm of SWE.

318   Similar snowpack loading and timing occurred across the Lake Tahoe basin at sites with similar

319   elevations (e.g., Mt. Rose/Squaw Valley, Marlette Lake/Rubicon). Early season storms were

320   dominated by northerly wind patterns contributing substantial snowfall in the northeastern areas

321   of the Lake Tahoe basin and reducing the typical pattern of lower snow accumulation on the

322   eastern side of the basin due to the rain shadow effect of the Sierra Nevada crest (e.g., 2012-13

323   Mt. Rose/Squaw Valley SNOTEL data). These early storms were followed by three dry months

324   with very little accumulation for the rest of winter. The 2013-14 snow year experienced the

325   lowest snow accumulation of all three study years with minimal snowpack development

326   occurring until late season storms in March and April brought peak SWE storage up to

327   approximately 575 mm. Minimal snowpack development occurred at lower lake level elevations

328   (e.g. Tahoe City SNOTEL data) throughout the entire 2013-14 season.

3.2   Nitrogen

3.2.1   Nitrate (NO_3^--N)

Snowpack NO_3^--N concentrations ranged from 20 to 138 ug L^{-1} (n=49 cores), 14 to 98

ug L^{-1} (n=56 cores), and 28 to 62 ug L^{-1} (n=3 integrated snow pits) during 2011-12, 2012-13, and

2013-14, respectively. These values were comparable with previous measurements at the

Emerald Lake Watershed, a remote watershed in the southern Sierra Nevada (Williams et al.,

1995). During 2011-12 and 2012-13 (i.e. the two years with detailed spatial and temporal

sampling), no distinguishable temporal or spatial pattern was observed in either snowpack NO_3^--

N concentrations or loads (Figure 4). ANOVA results confirmed that snowpack NO_3^--N

concentrations were not statistically affected by elevation, location (i.e. east/west), or early

versus late season sampling (Table 1). Comparisons of wet deposition and integrated average

snow pit concentrations during the 2013-2014 snow year showed that snowpack NO_3^--N

concentrations were similar to volume-weighted wet deposition up to the date of snowpack

sampling (Figure 5). This result is similar to patterns observed by Clow et al. (2002) and

Williams and Melack (1991a) and may be indicative of wet deposition as the main source of

NO_3^--N deposition. For example, wintertime deposition of NO_3^--N in the Rockies was found to

be highly correlated to precipitation with little difference between snowpack and NADP

precipitation volume-weighted mean concentrations suggesting mainly wet deposition inputs

(Clow et al., 2002). Similarly, a study at the Emerald Lake Watershed identified that dry

deposition of NO_3^- was not an important contributor of total NO_3^- load in winter snowpack

(Williams and Melack, 1991a). Our study revealed that increased precipitation on the west side

of the Tahoe Basin during 2011-12 led to correspondingly greater NO_3^- loading; while, little

351 difference was seen during 2012-13 when precipitation totals throughout the basin were more

352 uniform.

353   Vertical snow pit profile patterns show large variability in NO_3^--N concentrations with

354 depth, e.g. decreasing concentrations below the top 30-40 cm (Figure 6). This variability

355 suggests pronounced in snowpack dynamics possibly driven by conversion, vertical transport, or

356 elution. In addition, several studies have shown significant wintertime dry deposition of NO_3^--N,

357 in particular close to highways and urban areas (Cape et al., 2004; Dasch and Cadle, 1986;

358 Kirchner et al., 2005). Therefore, the fact that wet deposition concentrations were very similar to

359 snowpack concentrations could be merely a coincidence and may not allow us to infer dry versus

360 wet deposition of NO_3^--N.

361   Previous studies have observed parallel concentration declines of SO_4^{2-} and NO_3^--N

362 during snowpack melt events due to similar early-season ionic pulses that lead to preferential

363 losses of nutrients and other ions (Bales et al., 1989; Harrington and Bales, 1998; Tranter et al.,

364 1986). In support of such potential losses, Figure 4 shows decreasing snowpack NO_3^-

365 concentrations in spring months, particularly in the second year, 2012-13, when sampling

366 captured the beginning of the melt season. Preferential mobilization of solutes during melt events

367 also has been shown to cause downward movement of solutes in the snowpack (Williams and

368 Melack, 1991b). Our vertical snow pit samples show highly variable distribution patterns with

369 depth (Figure 6), which may indicate insufficient temporal resolution of pit sampling to detect

370 vertical translocation. Similar early elution characteristics have been observed for NO_3^- and

371 SO_4^{2-} (Stottlemyer and Rutkowski, 1990; Williams and Melack, 1991b), and comparing volume-

372 weighted seasonal wet deposition concentrations of SO_4^{2-} and snowpack $SO4^{2-}$ concentrations

373 showed no large elution losses either (Figure 5). Our results suggest that Tahoe Basin snowpack

374   NO_3^- is subject to multiple inputs and complex in snowpack processes, and that potential losses

375   (such as during early ionic pulses) may be difficult to detect against additional surface (e.g., dry)

376   deposition processes without very detailed time- and depth-resolved snowpack measurements.

377   **3.2.2   Total Ammonia Nitrogen (TAN)**

378   Snowpack concentrations of TAN ranged from 16 to 104 ug L^{-1} (n=49 cores), 10 to 77

379   ug L^{-1} (n=56 cores), and 28 to 85 ug L^{-1} (n=3 integrated snow pits) during 2011-12, 2012-13, and

380   2013-14, respectively. Snowpack TAN concentrations are within the range of previous

381   measurements made in the Emerald Lake Watershed of California, where the amount of TAN

382   deposited within the seasonal snowpack accounted for approximately 90% of annual loading

383   (Williams et al., 1995).

384   Unlike NO_3^--N, TAN is known to deposit through both wet and dry pathways during

385   winter (Clow et al., 2002; Ingersoll et al., 2008). In our study, strong evidence for an important

386   role of TAN dry deposition can be inferred from the fact that snowpack TAN concentrations

387   doubled from the early (Dec-Feb) to the late (Mar-Apr) season in both 2011-12 and 2012-13

388   (Figure 4). ANOVA results confirmed significant differences in snowpack TAN concentrations

389   between early and late season snowpack sampling (Table 1, p=0.01). Increased late season TAN

390   concentration in snowpack is consistent with similar observations in the Rocky Mountains and

391   the Stubai Alps (Bowman, 1992; Kuhn, 2001). These increases were attributed to the onset of

392   agricultural production in upwind valleys, as well as increased dry deposition due to decreased

393   atmospheric stability and increased convection. Importantly, the late season increase in

394   snowpack TAN occurred in both years, even though no significant late season snowfall occurred

395   in 2012-13 (Figure 4). The patterns of increasing TAN concentration in late season snowpack

396   with no significant snowfall agree with previous research showing dry deposition as the

397   significant source of TAN deposition in the Sierra Nevada (Bytnerowicz and Fenn, 1996).

398   Large increases in NH_3 emissions from winter to spring have been measured upwind of

399   the Sierra Nevada in the San Joaquin Valley, CA and were attributed to increased agricultural

400   and livestock activities (Battye et al., 2003). Further support of snowpack TAN sourcing in the

401   San Joaquin Valley, was higher concentrations at west basin sites than east basin sites during

402   both 2011-12 and 2012-13. ANOVA results revealed a significant difference between the east

403   and west basin snowpack TAN concentrations (Table 1, p=0.03). This increase is likely due to

404   the west basin sites being closer in proximity to San Joaquin Valley agricultural activity allowing

405   for increased transport and deposition.

406   During the 2013-14 snow year, TAN concentrations were consistently higher (up to a

407   factor of 3) in volume-weighted wet deposition than integrated snow pit samples (Figure 5;

408   p=0.08, note low replicate of n=3). This increase of TAN further emphasizes the importance of

409   dry deposition of TAN to Tahoe Basin snowpack. During snowpack storage, TAN is known to

410   elute relatively late during melt events (Kuhn, 2001); however, other transformations such as

411   microbial conversion can lead to decreases and losses throughout the season. Snow pit depth

412   profile sampling shows a decrease in TAN concentrations with depth and therefore age (Figure

413   6). This decrease coincides with increases in organic N suggesting microbial conversion of

414   inorganic N to organic N. Despite these possible losses, the increase we observe between wet

415   deposition and snow pit concentrations indicates that the additional input of TAN from dry

416   deposition is large enough to exceed transformations that occur during snowpack storage.

417   Late season deposition doubled TAN snowpack loads prior to end-of-season melt. The

418   fate of snowpack TAN has been studied extensively through both watershed mass balance and

419   tracer-based research. For example, less than 1% of TAN stored in snowpack at Emerald Lake,

420   California reached the lake as TAN during melt and runoff (Williams and Melack, 1991b).

421   During a later study, however, snowmelt with isotopically labeled NH_3 was retained in the soils

422   during melt making it a possible contributor to future NO_3^- stream pulses after nitrification

423   (Williams et al., 1996). Current predictions show an increase in total N emissions during the next

424   half-century in the western United States due to large increases in agricultural and livestock NH_3

425   emissions (Fenn et al., 2003). Such increased emissions could result in significant additional

426   deposition loads of TAN to snowpack in the Sierra Nevada with the potential to alter ecosystem

427   nutrient dynamics.

428   **3.2.3   Organic Nitrogen**

429   Integrated snowpack organic N concentrations ranged from BDL (below detection limit)

430   to 211 ug L^{-1} in 2011-12 (n=49 cores), BDL to 253 ug L^{-1} in 2012-13 (n=56 cores), and 120 to

431   260 ug L^{-1} in 2013-14 (n=3 integrated snow pit). No dominant spatial or temporal patterns were

432   observed in snowpack organic N concentrations or loads for either 2011-12 or 2012-13 (Figure

433   4). ANOVA results supported this finding with no significant effects of location, elevation, or

434   early/late season on organic N concentrations (Table 1). A previous study found large variation

435   in wintertime deposition of organic N throughout the Rocky Mountain Range; accounting for

436   40% , 3%, and 50% of total N in wet deposition during January, February, and March,

437   respectively (Benedict et al., 2013). Deposition rates and patterns of organic N are difficult to

438   quantify due to the large number of compounds – including gaseous, particulate, and dissolved

439   phases – originating from local, regional, and global sources and subject to biological and

440   chemical transformations (Cape et al., 2011; Neff et al., 2002).

441   Overall, snowpack core samples collected during the 2011-12 and 2012-13 seasons

442   showed high fractions of organic N accounting for 49 ± 17% of total snowpack N on average.

443   Inorganic forms, TAN and NO_3^--N, accounted for 21 ± 10 and 29 ± 10%, respectively (Figure 7).

444   Research at a high elevation catchment in the Colorado Front Range identified organic N as an

445   important component in both wintertime wet deposition and stream export (Williams et al.,

446   2001), while data from a fourteen year study (WY1985-1998) in the Southern Sierra Nevada

447   reports that on average dissolved organic nitrogen (DON) accounted for 35% of total N (NH_4^+ +

448   NO_3^- + DON) in winter precipitation (Sickman et al., 2001). Comparison of volume-weighted wet

449   deposition and integrated snow pit concentrations showed higher concentrations (up to a factor

450   of 2.5) of organic N in the snowpack (Figure 5). Two possible sources could cause higher

451   concentrations of organic N in snowpack compared to wet deposition: snowpack microbial

452   conversion of inorganic N to organic N and dry deposition of organic N during storm-free

453   periods (Clement et al., 2012; Jones, 1999; Williams et al., 2001). Our measurements do not

454   allow for differentiation between the two possible sources of snowpack organic N; however

455   snow pit profile sampling shows coinciding decreases of inorganic N and increases in organic N

456   with snow pit depth and therefore age (Figure 6). One Arctic snowpack study found that

457   microbial-based N cycling was a dominant process explaining N species availability at the base

458   of the snowpack (Larose et al., 2013). We suggest that microbial uptake of inorganic N may be a

459   primary driver of the increasing snowpack organic N levels during storage. Overall, we observed

460   that the dominant form of N in Sierra Nevada snowpack during our study was organic N, and

461   propose that this large representation warrants detailed studies in regard to the sources, cycling,

462   and fate of organic N in the Sierra Nevada.

463   Concentrations and loads of total N in snowpack are apparently dependent on

464   contributions of both inorganic and organic forms; with respective differences in deposition

465   pathways (wet versus dry deposition), potential conversion processes (e.g., from inorganic to

466   organic forms), and different mobilization during elution sequences leading to large fluctuations

467   in both the concentration and spatial-temporal patterns of snowpack total N throughout the

468   season. Total N accumulation in Sierra Nevada snowpack shows strong interannual variability as

469   well as different representation of various N species.

470   **3.3   Phosphorus**

471   Snowpack TP concentrations ranged from 3 to 109 ug L^{-1} in 2011-12 (n=49 cores), 3 to

472   59 ug L^{-1} in 2012-13 (n=56 cores), and 10 to 41 ug L^{-1} in 2013-14 (n=3 integrated snow pits).

473   Figure 8 shows that the urban site in Incline Village at lake level had by far the highest snowpack

474   TP concentrations, ranging up to six times higher than any other snowpack concentration at

475   similar elevation (i.e. lake level). In comparison, the Thunderbird site, also at lake level, located

476   in a very remote setting just 10 km from Incline, had much lower P concentrations. Sources such

477   as fugitive dust from plowing, forest and agriculture biomass burning, and diesel engine

478   combustion have been identified as major sources of particulate-phase atmospheric P in

479   California (Alexis, 2001). Specifically in the Lake Tahoe basin, road dust has been identified as a

480   primary contributor of P input into Lake Tahoe (Dolislager et al., 2012), while another study

481   found significant P emissions from urban biomass burning (Zhang et al., 2013). Our patterns

482   suggest that urban areas in the Lake Tahoe basin are a major source area for P deposition to

483   snowpack during winter and spring.

484   Local and regional emissions are also relevant at larger scales, as evident in 2011-12,

485   where remote sites at eastern locations in the basin showed higher TP concentrations than

486   western sites. We propose that the large concentration of urban source sites at lake level

487   combined with the dominant west to east wind pattern led to increased deposition on the east side

488   of the basin. During 2012-13, no west-to-east increase in TP concentration was observed;

489   however, the strong influence of urban activity remained. It is unlikely that sources of P in the

490   basin changed between 2011-12 and 2012-13, and it is more likely that different deposition

491   patterns due to differences in snow accumulation, timing, and storm track directions caused this

492   change. Even though there was significantly higher P deposition on the east side of the basin

493   from urban influence, the relatively remote west basin snowpack still had TP concentrations of

494   11.8 ug L^{-1} on average. Diffuse regional P sources to the Tahoe Basin include both dust and

495   aerosol inputs. Particulate matter particles smaller than 10 μm in diameter (PM_{10}) are capable of

496   long-range transport, while larger particles have higher deposition velocities and decreased

497   transport (Vicars et al., 2010). Specifically, dust-derived inputs originate from geologic sources

498   and erosion from both agricultural and urban activity, while burning from both forest and

499   domestic fires contributes additional particulate matter in the form of ash and soot (Raison et al.,

500   1985). Differences in P deposition rates between the dry and wet seasons as well as spatial

501   patterns associated with wind direction and soil erosion vulnerability have been observed in the

502   southern Sierra; Ontario, Canada; and the Mediterranean (Brown et al., 2011; Morales-Baquero

503   et al., 2006; Vicars and Sickman, 2011).

504   Comparison of volume-weighted wet deposition and integrated snow pit concentrations

505   showed higher levels of TP (up to a factor of 5.8) in snowpack than wet deposition (Figure 5).

506   This increase further supports dry deposition as a primary input of snowpack P. Finally,

507   snowpack o-PO$_4$, the most bioavailable form of P (Dodds, 2003), accounted for $34 \pm 15\%$ of

508   snowpack TP; similar to previous work in the Lake Tahoe region that estimated approximately

509   40% of TP in atmospheric deposition was in a bioavailable form (LTTMDL, 2010).

510   Low P levels in parent material make high elevation watersheds of the Sierra Nevada,

511   sensitive to the effects of external P inputs (Melack and Stoddard, 1991; White et al., 1999).

512   Further research, however, has shown that extractable P levels of parent material strongly

513   influence P adsorption. The very high extractable P levels in granitic soils in the Sierra Nevada

514   lead to low P adsorption potentials, while the low extractable P levels and sesquioxide content of

515   volcanic soils in the Sierra Nevada increase adsorption (Johnson et al., 1997). Approximately

516   two-thirds of the Lake Tahoe basin parent material is granitic and one-third is volcanic

517   (LTTMDL, 2008), making soil adsorption potentials of atmospherically deposited P throughout

518   the watershed highly variable with location. Along with N, P levels directly control algal

519   production within aquatic ecosystems, and algal production is a key reason for declining clarity

520   in Lake Tahoe (Dolislager, 2006). In particular, the high snowpack concentrations at urban

521   locations near the lake may cause a significant influx of P into Lake Tahoe during melt.

522   **3.4   Mercury**

523   Snowpack THg concentrations ranged from 0.81 to 7.58 ng L^{-1} in 2011-12 (n=49 cores),

524   0.97 to 5.96 ng L^{-1} in 2012-13 (n=56 cores), and 3.28 to 7.56 ng L^{-1} in 2013-14 (n=3 integrated

525   snow pits). The Tahoe Basin average snowpack core THg concentration for 2011-12 and 2012-

526   13 was 2.56 ± 1.3 ng L^{-1}. Observed THg concentrations are slightly lower, but within range of

527   the end-of-season average snowpack concentration measured during a watershed Hg balance

528   study in 2009 at Sagehen Creek, CA (i.e. 3.3 ng L^{-1}; Fain et al., 2011), a remote watershed

529   located only 32 km north of the Tahoe Basin. Particulate Hg was the dominant form of Hg within

530   Tahoe snowpack accounting for 76.1 ± 8.7, 70.3 ± 13.4, and 87.1 ± 4.7 of THg on average

531   during 2011-12, 2012-13 and 2013-14, respectively. The large percentage of particulate Hg in

532   the snowpack agrees with previous findings from a study in Canada that saw a post-depositional

533   increase in particulate associated Hg from approximately 50% to 70% (Poulain et al., 2007). This

534   study attributed particulate throughfall and photochemical induced emission as the main causes

535   of the speciation shift and also noted strong differences in snowpack Hg concentrations between

536   open and forested areas which were attributed to throughfall contributions from tree canopies as

537   well as shading reducing photochemical evasion.

538   Snowpack coring revealed no dominant temporal or spatial patterns in THg or DHg

539   deposition with ANOVA results showing no significant effects of season (i.e., early versus late)

540   or location (i.e., east versus west; Table 1). The lack of spatial trends suggests that global

541   background atmospheric pollution, rather than specific point sources such as urban areas, as the

542   main source of snowpack Hg in the Lake Tahoe basin. Mercury's long atmospheric lifetime and

543   global circulation allow for diffuse deposition to this relatively remote mountain region (Fain et

544   al., 2011; Schroeder and Munthe, 1998); and the majority of large snowfall events in the Sierra

545   Nevada originate as large-scale convection cells in the eastern Pacific and travel hundreds of

546   kilometers before reaching the Tahoe Basin (O'Hara et al., 2009). To our knowledge, few point

547   sources for Hg emission exist within the Lake Tahoe basin, although one study within the basin

548   reported that significant amounts of particulate Hg are emitted from wildfires (Zhang et al.,

549   2013) and found increased levels of particulate Hg in urban areas of the Lake Tahoe basin.

550   Both THg and DHg concentrations in the snowpack significantly increased with elevation

551   in the basin (Table 1; $p < 0.05$). This finding is in contrast to an expected "washout effect" which

552   causes declines in Hg precipitation concentrations with storm duration and magnitude (Poissant

553   and Pilote, 1998). King and Simpson (2001) observed that approximately 85% of photochemical

554   reactions occur in the top 10 cm of the snowpack. It is possible that the increase in Hg

555   concentration with elevation is due to decreased light penetration relative to snowpack depth and

556   reduced photochemical re-emission, as increased elevation leads to the formation of a deeper,

557   denser snowpack. In support of this notion is a significant positive correlation between integrated

558   snowpack THg concentration and total SWE (slope: 0.002 [ng L^{-1} SWE (mm) $^{-1}$]; p-value:

559   <0.05), as well as strong elevation gradients in total snowpack Hg pools. In agreement, total

560   snowpack Hg loading was significantly higher in 2012-13 than in 2011-12 (Table 1; p<0.01) in

561   accordance with higher overall SWE. Evidence for surface-based photochemical losses of Hg are

562   lower concentrations of Hg in upper snowpack layers (Figure 6). Declines in Hg concentrations

563   between cumulative wet deposition and integrated snowpack content were mainly driven by

564   DHg, with up to 4.5 times lower concentrations observed in integrated snow pit samples than

565   volume weighted wet deposition (Figure 5). Aside from photochemical losses, it is possible that

566   vertical patterns are co-determined by vertical movement and solute transport of Hg. Previous

567   studies have reported Hg pulses in runoff during snowmelt events (Schuster et al., 2008). In

568   addition, sorption processes could lead to conversion between DHg and particulate Hg and

569   changes snowpack Hg speciation. The combination of strong precipitation gradients and

570   increased THg concentration with SWE lead to large spatial variability in the total snowpack Hg

571   pools in mountainous areas. A previous study noted relationships between soil Hg content and

572   elevation (Gunda and Scanlon, 2013), possibly attributable to precipitation gradients, while

573   another study found that soil Hg storage was positively correlated to total precipitation across

574   multiple study sites, but attributed these effects to ecological processes such as increased plant

575   productivity and carbon accumulation (Obrist et al., 2009; Obrist et al., 2011).

576   Photochemical reduction and volatile reemission of gaseous Hg during snowpack storage

577   has been widely studied and is known to account for losses of up to 50% from that measured in

578   initial deposition (Fain et al., 2007; Fain et al., 2011; Lalonde et al., 2002; Mann et al., 2011;

579   Poulain et al., 2007). However, at the end of the season, we still observed substantial

580   concentrations of Hg left in the snowpack (e.g. ranging from ~55 to ~105% of volume-weighted

581   wet deposition) that will be subject to melt and infiltration into the watershed. In addition to the

582   declines of DHg during storage, an increase in particulate Hg was observed in two of the three

583   comparisons of snow pit and wet deposition samples (Figure 5) and it is possible that

584   photochemical losses from snow are in part offset by gaseous-dry deposition and particulate

585   throughfall during storm free periods.

586   A study at the nearby Sagehen Creek, California watershed quantified that only 4% of

587   total annual Hg wet deposition was exported from the watershed in stream water and identified

588   soil uptake and storage as well as photochemical re-emission as the major sinks of

589   atmospherically deposited Hg (Fain et al., 2011). While soil uptake serves as a buffer delaying

590   the transport of upland wet deposition to streams, sediment core analyses still showed that

591   upland watershed contributions (i.e., through soil erosion and sediment flux) are significant

592   contributors of Hg input to lakes even under relatively low watershed to lake area ratios as in the

593   Lake Tahoe basin (extrapolated to 42% contributions when using relationships presented by

594   Lorey and Driscoll, 1999). Snowpack-based Hg input to the watershed, therefore, is expected to

595   contribute to lake water quality through erosion and sediment-based influx, albeit delayed in time

596   and closely linked to soil Hg pools and mobilization.

597 **3.5   Basin-wide Loading Estimates**

598   Declines in Lake Tahoe water quality have been observed during the last 50 years (Sahoo

599 et al., 2010; Schuster and Grismer, 2004). Specifically, secchi depths, a measure of lake

600 transparency, have decreased from approximately 30.5 m to 21.3 m since the 1960s (TERC,

601 2011). Eutrophication from atmospheric and terrestrial nitrogen (N) and phosphorus (P) inputs as

602 well as light scattering by particulate inputs are the main causes of this decline (Jassby et al.,

603 2003; Swift et al., 2006). Most previous studies in the Lake Tahoe basin have focused on direct

604 atmospheric deposition to the lake surface (Dolislager et al., 2012; NADP, 2012), and little

605 information is available on snowpack-based loading for the surrounding upland watershed. The

606 surrounding land surface covers 814 km^2 of the 1,310 km^2 Lake Tahoe watershed. Direct

607 atmospheric inputs to the lake surface are estimated to contribute 55 and 15% of total N and P,

608 respectively (TERC, 2011). Stream monitoring data show that upon snowmelt, Lake Tahoe

609 receives large pulses of N and P (Goldman et al., 1989; Hatch et al., 1999), which together

610 control algal production within the basin's aquatic ecosystems contributing to the decline in

611 clarity in Lake Tahoe during the last 50 years (Dolislager, 2006). Although much of snowpack-

612 based chemical loads may not directly enter Lake Tahoe upon melt, snowpack loads are

613 important for terrestrial chemical budgets. For example, nutrient rich O-horizon runoff –

614 measuring as high as 87.2 mg L^{-1} NH$_4$-N, 95.4 mg L^{-1} NO$_3$-N, and 24.4 mg L^{-1} PO$_4$-P – has been

615 observed in Lake Tahoe forests during snowmelt events due to leaching from the forest litter

616 layer (Miller et al., 2005). In order to relate peak snowpack nutrient and pollutant loading to

617 previous terrestrial and lake chemical budgets, we here estimate average peak basin-wide

618 snowpack chemical storage using the peak SWE decadal average from 2000-2011(Figure 2a).

619 While canopy effects on total snow accumulation are incorporated in this estimate through the

620   SWE reconstruction model, we did not include forest canopy effects on deposition and chemical

621   dynamics as our snowpack measurements were limited to open, canopy-free locations.

622   Deposition and snowpack dynamic processes in forests are known to show substantial

623   differences compared to canopy-free locations, including increased dry deposition, throughfall

624   deposition, or different photochemical processes (Poulain et al., 2007; Tarnay et al., 2002). In

625   order to be able to compare different locations across the basin, we selected to not consider forest

626   canopy locations and data on chemical dynamics, deposition, and storage are limited to open

627   areas. The estimated deposition loads, therefore, are based on deposition and snowpack storage

628   measured in canopy-free locations and could be different when effects of canopies and other

629   forest processes were incorporated.

630

631   ### 3.5.1   Nitrogen

632   Snowpack NO_3^--N loading was highly dependent on snow accumulation, but

633   concentrations showed little temporal or spatial trends throughout the Lake Tahoe basin (Table

634   1). To calculate basin-wide NO_3^--N loads, we therefore multiplied the two-year seasonal average

635   concentration (47.1 ug L^{-1}) by the decadal average reconstructed SWE. Basin-wide NO_3^--N

636   loading estimates (mass area^{-1}) thus reflect snowpack accumulation patterns (i.e., SWE) with the

637   highest loading occurring on the west-side of the basin at high elevations, up to approximately

638   1 kg ha^{-1}, and decreasing toward the east and with lower elevations due to lower SWE

639   accumulation. Average annual snowpack NO_3^--N storage for the Lake Tahoe basin is estimated

640   at 28.7 metric tons (t).

641   Unlike NO_3^--N, snowpack TAN loading in the Lake Tahoe basin showed strong spatial

642   and temporal trends. Late season deposition effectively doubled snowpack TAN concentrations

643   with significantly higher concentrations on the west side of the basin than the east side (Table 1).

644   Due to these relationships, we applied the March and April (peak SWE generally occurs during

645   March and April in the Lake Tahoe basin) average snowpack TAN concentration from the east

646   and west basin sites to the reconstructed SWE data (western sites: 57.9 ug L^{-1}, eastern sites:

647   41.6 ug L^{-1}) to scale up snowpack TAN loading to the whole basin. Modeled estimates,

648   therefore, show greater TAN accumulation on the western side of the basin with highest loading

649   occurring at high elevations in the west (up to approximately 1.2 kg ha^{-1}) due to the combination

650   of both large snow accumulation and proximity to upwind sources. Our estimate of average

651   annual basin-wide accumulation of TAN within the basin's snowpack is 30.5 t.

652   Snowpack organic N concentrations throughout each sampling season were variable and

653   showed no clear temporal or spatial trends (Table 1). Applying the average concentration of

654   88.7 ug L^{-1} from all snowpack samples throughout both years produced an annual estimate of

655   54.1 t of organic N stored within the basin's snowpack.

656   Average annual snowpack N storage for the Lake Tahoe watershed – calculated as the

657   sum of NO_3^--N, TAN, and organic N – totaled 113 t (Figure 2b). Inorganic and organic forms

658   made up 52% and 48% of total N, respectively. TAN and NO_3^--N accounted for 27% and 25% of

659   total snowpack N, respectively. Annual N loading estimates for Lake Tahoe (from terrestrial

660   runoff and direct atmospheric deposition) were previously estimated to be 397 t yr^{-1}, with 218 t

661   yr^{-1} originating from atmospheric sources depositing directly on the lake's surface (LTTMDL,

662   2010). With the caveat that estimation methods differed, snowpack N storage estimates from our

663   study represent approximately 28% of the lake's total N budget. Comparing our estimates to the

664   179 t of N that originates from runoff and terrestrial sources, annual snowpack N storage would

665   replenish approximately 63% of this flux.

666   **3.5.2   Phosphorus**

667   Snowpack P accumulation in the Lake Tahoe basin was strongly related to proximity to

668   urban sources, as well as transport along the dominant westerly winds throughout the basin. This

669   dependence caused the highest P concentration in the snowpack to occur in developed areas and

670   higher concentrations across east basin sites than remote west basin sites (Table 1). Applying

671   different P concentrations based on degree of urbanization (see section 2.5), highest P loading

672   (up to approximately 0.4 kg ha^{-1}) occurs, therefore, at high elevations with significant impacts of

673   urban emissions (i.e., northeastern and southern locations influenced by Incline Village, Nevada

674   and South Lake Tahoe, California). The basin-wide average TP storage estimated during this

675   study of 0.11 kg ha^{-1} is more than double the average snowpack storage reported for the ELW

676   watershed (0.04 kg ha^{-1}; Sickman et al., 2003) and reflects increased urbanization within the

677   Tahoe Basin. Homyak et al. (2014) estimate that atmospheric deposition has contributed up to

678   31% of P accumulation and loss in soils and runoff since deglaciation of the Emerald Lake

679   Watershed. The higher snowpack loading rates estimated during this study indicate that

680   atmospheric deposition could be the primary supplier of excess P input to the Tahoe Basin.

681   Overall, we estimate a peak P load of approximately 9.3 t of P stored annually in Lake

682   Tahoe basin snowpack (Figure 2c). Previous pollutant loading studies for Lake Tahoe estimated

683   that approximately 46 t of P enters the lake each year with approximately 39 t of the annual

684   budget originating from land-based sources (LTTMDL, 2010). Annual snowpack TP storage

685   estimates, therefore, could represent approximately 20% of total P input into Lake Tahoe each

686   year.

3.5.3   Mercury

Similar to NO_3^--N, snowpack THg concentrations showed little temporal or east to west variation (Table 1). However, THg concentrations were positively related to total SWE (slope: 0.00201 [ng L^{-1} mm^{-1}]; p-value: 0.016). Applying this relationship to reconstructed SWE data produced the following THg distribution throughout the Lake Tahoe basin (Figure 2d); THg loading throughout the basin followed strong elevation gradients, with the uppermost areas of the basin receiving the highest concentrations and total loading (up to approximately 125 mg ha^{-1}) due to increased snow accumulation. Average annual snowpack THg concentration and loading for the Lake Tahoe watershed was 3.6 ng L^{-1} and 30 mg ha^{-1}, respectively, based on the decadal SWE accumulation average of 750 mm. We do not have any previous data on Hg deposition to this basin, but these values are comparable to the 3.3 ng L^{-1} average snowpack Hg concentration and 13 mg ha^{-1} peak snowpack loading from the Sagehen Creek watershed in 2009 when snowpack accumulation was approximately 400 mm (Fain et al., 2011). The basin-wide estimate of THg stored within the annual snowpack was 1166.2 g. Snow-based Hg fluxes estimated during this study fall within range of measurements (3.36 mg ha^{-1} yr^{-1} to 36 mg ha^{-1} yr^{-1}) taken at seven national parks throughout western North America during the Western Airborne Contaminants Assessment Project (WACAP), which found fish Hg levels above the human consumption threshold even at sites with relatively low Hg deposition (Landers et al., 2008).

4   Conclusions

In summary, spatial and temporal pattern analyses suggest that out-of-basin sources were important for Hg and TAN, while in-basin sources controlled P deposition, with the highest concentrations measured near urban areas, exceeding remote location concentrations by up to a factor of 6. Snowpack NO_3^--N concentrations were relatively uniform throughout the basin

710   indicating out-of-basin sourced wet deposition as a primary input; however high variability in

711   snow pit vertical concentrations suggests additional inputs and in snowpack transport and

712   conversion processes. Second, increased NH_3 emissions from the San Joaquin Valley and

713   increased atmospheric vertical mixing during the onset of spring likely led to dry deposition-

714   based increases of snowpack TAN during March and April, effectively doubling snowpack TAN

715   concentrations prior to melt. Third, chemical speciation showed that organic N in the Lake Tahoe

716   snowpack accounted for 48% of total N on average with possible microbial conversion leading to

717   higher enhanced organic N levels in deeper older snowpack. Fourth, particulate Hg was the

718   dominant form of Hg (78% on average) within Tahoe snowpack and concentrations of both THg

719   and DHg increased with elevation and SWE likely due to decreased light penetration and

720   reduced photochemical reemission in deeper snowpack. Finally, basin-wide modeling estimates

721   indicated that Lake Tahoe basin snowpack acts as a substantial reservoir in which atmospheric

722   nutrients and pollutants accumulated throughout winter and spring. Estimates of basin-wide

723   annual snowpack mass loading showed accumulation of N, P, and Hg yielding 113 t of N, 9.3 t

724   of P, and 1166.2 g of Hg. Further research should focus on quantifying the relationship between

725   snowmelt processes and stream and groundwater input, and address the substantial amount of

726   organic N stored within the basin's snowpack.

738   **6   References**

739   Alexis, A., A. Delao, C. Garcia, M. Nystrom, and K Rosenkranz.: The 2001 California almanac of emissions
740   and air quality. California Air Resources Board., 2001. 2001.
741   Bales, R. C., Davis, R. E., and Stanley, D. A.: Ion elution through shallow homogeneous snow, Water
742   Resour. Res., 25, 1869-1877, 1989.
743   Battye, W., Aneja, V. P., and Roelle, P. A.: Evaluation and improvement of ammonia emissions
744   inventories, Atmos. Environ., 37, 3873-3883, 2003.
745   Benedict, K. B., Carrico, C. M., Kreidenweis, S. M., Schichtel, B., Malm, W. C., and Collett, J. L.: A seasonal
746   nitrogen deposition budget for Rocky Mountain National Park, Ecol. Appl., 23, 1156-1169, 2013.
747   Berg, N. H.: Ion elution and release from deep snowpacks in the central Sierra-Nevada, California, Water
748   Air Soil Pollut., 61, 139-168, 1992.
749   Bowman, W. D.: Inputs and storage of nitrogen in winter snowpack in an alpine ecosystem, Arct. Alp.
750   Res., 24, 211-215, 1992.
751   Brooks, P., Williams, M., and Schmidt, S.: Microbial activity under alpine snowpacks, Niwot Ridge,
752   Colorado, Biogeochemistry, 32, 93-113, 1996.
753   Brooks, P. D. and Williams, M. W.: Snowpack controls on nitrogen cycling and export in seasonally snow-
754   covered catchments, Hydrol. Process., 13, 2177-2190, 1999.
755   Brown, L. J., Taleban, V., Gharabaghi, B., and Weiss, L.: Seasonal and spatial distribution patterns of
756   atmospheric phosphorus deposition to Lake Simcoe, ON, J. Gt. Lakes Res., 37, 15-25, 2011.
757   Bytnerowicz, A. and Fenn, M. E.: Nitrogen deposition in California forests: A review, Environ. Pollut., 92,
758   127-146, 1996.
759   CADWR: http://cdec.water.ca.gov/snow/current/snow/index.html, 2014.
760   Cape, J. N., Cornell, S. E., Jickells, T. D., and Nemitz, E.: Organic nitrogen in the atmosphere — Where
761   does it come from? A review of sources and methods, Atmospheric Research, 102, 30-48, 2011.
762   Cape, J. N., Tang, Y. S., van Dijk, N., Love, L., Sutton, M. A., and Palmer, S. C. F.: Concentrations of
763   ammonia and nitrogen dioxide at roadside verges, and their contribution to nitrogen deposition,
764   Environ. Pollut., 132, 469-478, 2004.
765   Clement, J. C., Robson, T. M., Guillemin, R., Saccone, P., Lochet, J., Aubert, S., and Lavorel, S.: The effects
766   of snow-N deposition and snowmelt dynamics on soil-N cycling in marginal terraced grasslands in the
767   French Alps, Biogeochemistry, 108, 297-315, 2012.
768   Clow, D. W., Ingersoll, G. P., Mast, M. A., Turk, J. T., and Campbell, D. H.: Comparison of snowpack and
769   winter wet-deposition chemistry in the Rocky Mountains, USA: implications for winter dry deposition,
770   Atmos. Environ., 36, 2337-2348, 2002.

771 Dasch, J. M. and Cadle, S. H.: Dry deposition to snow in an urban area, Water Air Soil Pollut, 29, 297-308,
772 1986.
773 Dodds, W. K.: Misuse of inorganic N and soluble reactive P concentrations to indicate nutrient status of
774 surface waters, Journal of the North American Benthological Society, 22, 171-181, 2003.
775 Dolislager, L., Lashgari, A., Pederson, J. and VanCuren, J.: Lake Tahoe Atmospheric Depositon Study
776 (LTADS), Atmospheric Processes Research Section Research Division, Air Resources Board, California
777 Environmental Protection Agency., 2006. 2006.
778 Dolislager, L. J., VanCuren, R., Pederson, J. R., Lashgari, A., and McCauley, E.: A summary of the Lake
779 Tahoe Atmospheric Deposition Study (LTADS), Atmos. Environ., 46, 618-630, 2012.
780 EPA: Method 1631, Revision E: Mercury in Water by Oxidation, Purge and Trap, and Cold Vapor Atomic
781 Fluorescence Spectrometry. Water, O. o. (Ed.), Washington DC 20460, 2002.
782 EPA: Methods for Chemical Analysis of Water and Wastes. Environmental Monitoring and Support
783 Laboratory, O. o. R. a. D. (Ed.), Cincinnati, Ohio 45468, 1979.
784 EPA: Methods for the Determination of Inorganic Substances in Environmental Samples. Development,
785 O. o. R. a. (Ed.), Washington D.C., 20460, 1993.
786 Fain, X., Grangeon, S., Bahlmann, E., Fritsche, J., Obrist, D., Dommergue, A., Ferrari, C. P., Cairns, W.,
787 Ebinghaus, R., Barbante, C., Cescon, P., and Boutron, C.: Diurnal production of gaseous mercury in the
788 alpine snowpack before snowmelt, J. Geophys. Res.-Atmos., 112, 2007.
789 Fain, X., Obrist, D., Pierce, A., Barth, C., Gustin, M. S., and Boyle, D. P.: Whole-watershed mercury
790 balance at Sagehen Creek, Sierra Nevada, CA, Geochim. Cosmochim. Acta, 75, 2379-2392, 2011.
791 Fenn, M. E., Haeuber, R., Tonnesen, G. S., Baron, J. S., Grossman-Clarke, S., Hope, D., Jaffe, D. A.,
792 Copeland, S., Geiser, L., Rueth, H. M., and Sickman, J. O.: Nitrogen emissions, deposition, and monitoring
793 in the western United States, Bioscience, 53, 391-403, 2003.
794 Fierz, C. A., R.L.; Durand, Y.; Etchevers, P.; Greene, E.; McClung, D.M.; Nishimura, K.; Satyawali, P.K.;
795 Sokratov, S.A.: The International Classification for Seasonal Snow on the Ground (ICSSG), International
796 Association of Cryospheric Sciences, 90 pp., 2009.
797 Fram, M. S., Belitz, K.,: Groundwater Quality in the Tahoe and Martis Basins, California: U.S. Geologic
798 Survey Fact Sheet., 2011. 4, 2011.
799 Galbavy, E. S., Anastasio, C., Lefer, B., and Hall, S.: Light penetration in the snowpack at Summit,
800 Greenland: Part 2 nitrate photolysis, Atmos. Environ., 41, 5091-5100, 2007.
801 Goldman, C. R., Jassby, A., and Powell, T.: Interannual fluctuations in primary productions-
802 Meteorological forcing at 2 subalpine lakes Limnol. Oceanogr., 34, 310-323, 1989.
803 Gunda, T. and Scanlon, T. M.: Topographical Influences on the Spatial Distribution of Soil Mercury at the
804 Catchment Scale, Water Air Soil Pollut., 224, 2013.
805 Halsall, C. J.: Investigating the occurrence of persistent organic pollutants (POPs) in the arctic: their
806 atmospheric behaviour and interaction with the seasonal snow pack, Environmental pollution (Barking,
807 Essex : 1987), 128, 163-175, 2004.
808 Harrington, R. and Bales, R. C.: Interannual, seasonal, and spatial patterns of meltwater and solute fluxes
809 in a seasonal snowpack, Water Resour. Res., 34, 823-831, 1998.
810 Hatch, L. K., Reuter, J. E., and Goldman, C. R.: Daily phosphorus variation in a mountain stream, Water
811 Resour. Res., 35, 3783-3791, 1999.
812 Homyak, P. M., Sickman, J. O., and Melack, J. M.: Pools, transformations, and sources of P in high-
813 elevation soils: Implications for nutrient transfer to Sierra Nevada lakes, Geoderma, 217–218, 65-73,
814 2014.
815 Ingersoll, G. P., Mast, M. A., Campbell, D. H., Clow, D. W., Nanus, L., and Turk, J. T.: Trends in snowpack
816 chemistry and comparison to National Atmospheric Deposition Program results for the Rocky
817 Mountains, US, 1993-2004, Atmos. Environ., 42, 6098-6113, 2008.

818   Jacobi, H. W. and Hilker, B.: A mechanism for the photochemical transformation of nitrate in snow, J.
819   Photochem. Photobiol. A-Chem., 185, 371-382, 2007.
820   Jassby, A. D., Reuter, J. E., Axler, R. P., Goldman, C. R., and Hackley, S. H.: Atmospheric deposition of
821   nitrogen and phosphorus in the annual nutrient load of Lake Tahoe (California Nevada), Water Resour.
822   Res., 30, 2207-2216, 1994.
823   Jassby, A. D., Reuter, J. E., and Goldman, C. R.: Determining long-term water quality change in the
824   presence of climate variability: Lake Tahoe (USA), Can. J. Fish. Aquat. Sci., 60, 1452-1461, 2003.
825   Jones, H. G.: The ecology of snow-covered systems: a brief overview of nutrient cycling and life in the
826   cold, Hydrol. Process., 13, 2135-2147, 1999.
827   King, M. D. and Simpson, W. R.: Extinction of UV radiation in Arctic snow at Alert, Canada (82°N), Journal
828   of Geophysical Research: Atmospheres, 106, 12499-12507, 2001.
829   Kirchner, M., Jakobi, G., Feicht, E., Bernhardt, M., and Fischer, A.: Elevated NH3 and NO2 air
830   concentrations and nitrogen deposition rates in the vicinity of a highway in Southern Bavaria, Atmos.
831   Environ., 39, 4531-4542, 2005.
832   Kuhn, M.: The nutrient cycle through snow and ice, a review, Aquat. Sci., 63, 150-167, 2001.
833   Lalonde, J. D., Poulain, A. J., and Amyot, M.: The role of mercury redox reactions in snow on snow-to-air
834   mercury transfer, Environ. Sci. Technol., 36, 174-178, 2002.
835   Landers, D. H., S.L. Simonich, D.A. Jaffe, L.H. Geiser, D.H. Campbell, A.R. Schwindt,, C.B. Schreck, M. L. K.,
836   W.D. Hafner, H.E. Taylor, K.J. Hageman, S. Usenko, L.K., and Ackerman, J. E. S., N.L. Rose, T.F. Blett, and
837   M.M. Erway.: The Fate, Transport, and Ecological Impacts of Airborne Contaminants in Western Nation
838   Parks (USA), EPA/600/R-07/138. U.S. Environmental Protection Agency, Office of Research

839   and Development, NHEERL, Western Ecology Division, Corvallis, Oregon., 2008.
840   Larose, C., Dommergue, A., and Vogel, T. M.: Microbial nitrogen cycling in Arctic snowpacks,
841   Environmental Research Letters, 8, 035004, 2013.
842   Lorey, P. and Driscoll, C. T.: Historical trends of mercury deposition in Adirondack lakes, Environ. Sci.
843   Technol., 33, 718-722, 1999.
844   LTTMDL: Lake Tahoe TMDL Pollutant Reduction Opportunity Report, California Water Boards; Nevada
845   Division of Environmental Protection, 2008.
846   LTTMDL: Lake Tahoe Total Maximum Daily Load Report 2010. 2010.
847   Mann, E., Meyer, T., Mitchell, C. P. J., and Wania, F.: Mercury fate in ageing and melting snow:
848   Development and testing of a controlled laboratory system, J. Environ. Monit., 13, 2695-2702, 2011.
849   McDaniel, M. R.: Semivolatile Organic Compounds in Snowmobile Emissions and in the Snowpack and
850   Surface Water in Blackwood Canyon, Lake Tahoe, CA, 3566275 Ph.D., University of Nevada, Reno, Ann
851   Arbor, 137 pp., 2013.
852   Melack, J. M. and Stoddard, J. L.: Sierra Nevada in D.F. Charles (ed.) Acidic Deposition and Aquatic
853   Ecosystems: Regional Case Studies, Springer-Verlag, New York, 1991.
854   Miller, W. W., Johnson, D. W., Denton, C., Verburg, P. S. J., Dana, G. L., and Walker, R. F.: Inconspicuous
855   nutrient laden surface runoff from mature forest Sierran watersheds, Water Air Soil Pollut., 163, 3-17,
856   2005.
857   Morales-Baquero, R., Pulido-Villena, E., and Reche, I.: Atmospheric inputs of phosphorus and nitrogen to
858   the southwest Mediterranean region: Biogeochemical responses of high mountain lakes, Limnol.
859   Oceanogr., 51, 830-837, 2006.
860   NADP: National Atmospheric Deposition Program (NADP); National Trends Network., 2012.
861   Neff, J., Holland, E., Dentener, F., McDowell, W., and Russell, K.: The origin, composition and rates of
862   organic nitrogen deposition: A missing piece of the nitrogen cycle?, Biogeochemistry, 57-58, 99-136,
863   2002.
864   NRCS: http://www.wcc.nrcs.usda.gov/snow/, 2013.

865   O'Hara, B. F., Kaplan, M. L., and Underwood, S. J.: Synoptic Climatological Analyses of Extreme Snowfalls
866   in the Sierra Nevada, Weather Forecast., 24, 1610-1624, 2009.
867   Obrist, D., Johnson, D. W., and Lindberg, S. E.: Mercury concentrations and pools in four Sierra Nevada
868   forest sites, and relationships to organic carbon and nitrogen, Biogeosciences, 6, 765-777, 2009.
869   Obrist, D., Johnson, D. W., Lindberg, S. E., Luo, Y., Hararuk, O., Bracho, R., Battles, J. J., Dail, D. B.,
870   Edmonds, R. L., Monson, R. K., Ollinger, S. V., Pallardy, S. G., Pregitzer, K. S., and Todd, D. E.: Mercury
871   Distribution Across 14 US Forests. Part I: Spatial Patterns of Concentrations in Biomass, Litter, and Soils,
872   Environ. Sci. Technol., 45, 3974-3981, 2011.
873   Painter, T. H., Rittger, K., McKenzie, C., Slaughter, P., Davis, R. E., and Dozier, J.: Retrieval of subpixel
874   snow covered area, grain size, and albedo from MODIS, Remote Sensing of Environment, 113, 868-879,
875   2009.
876   Poissant, L. and Pilote, M.: Mercury concentrations in single event precipitation in southern Quebec, Sci.
877   Total Environ., 213, 65-72, 1998.
878   Poulain, A. J., Roy, V., and Amyot, M.: Influence of temperate mixed and deciduous tree covers on Hg
879   concentrations and photoredox transformations in snow, Geochim. Cosmochim. Acta, 71, 2448-2462,
880   2007.
881   Raison, R. J., Khanna, P. K., and Woods, P. V.: Mechanisms of element transfer to the atmosphere during
882   vegetation fires Can. J. For. Res.-Rev. Can. Rech. For., 15, 132-140, 1985.
883   Rittger, K.: Spatial estimates of snow water equivalent in the Sierra Nevada, Ph.D. Thesis, Unversity of
884   California, Santa Barbara, Santa Barbara, 2012. 225, 2012.
885   Rittger, K., Painter, T. H., and Dozier, J.: Assessment of methods for mapping snow cover from MODIS,
886   Advances in Water Resources, 51, 367-380, 2013.
887   Rittger, K. K., A.; Dozier, J.: Topographic Distribution of Snow Water Equivalent in the Sierra Nevada,
888   Proceedings, Western Snow Conference 79, 37-46, 2011.
889   Rohrbough, J. A., Davis, D. R., and Bales, R. C.: Spatial variability of snow chemistry in an alpine
890   snowpack, southern Wyoming, Water Resour. Res., 39, 2003.
891   Rothlisberger, R., Hutterli, M. A., Wolff, E. W., Mulvaney, R., Fischer, H., Bigler, M., Goto-Azuma, K.,
892   Hansson, M. E., Ruth, U., Siggaard-Andersen, M. L., and Steffensen, J. P.: Nitrate in Greenland and
893   Antarctic ice cores: a detailed description of post-depositional processes. In: Annals of Glaciology, Vol
894   35, Wolff, E. W. (Ed.), Annals of Glaciology-Series, Int Glaciological Soc, Cambridge, 2002.
895   Sahoo, G. B., Schladow, S. G., and Reuter, J. E.: Effect of sediment and nutrient loading on Lake Tahoe
896   optical conditions and restoration opportunities using a newly developed lake clarity model, Water
897   Resour. Res., 46, 2010.
898   Schroeder, W. H. and Munthe, J.: Atmospheric mercury - An overview, Atmos. Environ., 32, 809-822,
899   1998.
900   Schuster, P. F., Shanley, J. B., Marvin-Dipasquale, M., Reddy, M. M., Aiken, G. R., Roth, D. A., Taylor, H.
901   E., Krabbenhoft, D. P., and DeWild, J. F.: Mercury and Organic Carbon Dynamics During Runoff Episodes
902   from a Northeastern USA Watershed, Water Air Soil Pollut, 187, 89-108, 2008.
903   Schuster, S. and Grismer, M. E.: Evaluation of water quality projects in the Lake Tahoe basin, Environ.
904   Monit. Assess., 90, 225-242, 2004.
905   Sickman, J. O., Leydecker, A., and Melack, J. M.: Nitrogen mass balances and abiotic controls on N
906   retention and yield in high-elevation catchments of the Sierra Nevada, California, United States, Water
907   Resour. Res., 37, 1445-1461, 2001.
908   Sickman, J. O., Melack, J. M., and Clow, D. W.: Evidence for nutrient enrichment of high-elevation lakes
909   in the Sierra Nevada, California, Limnol. Oceanogr., 48, 1885-1892, 2003.
910   Stottlemyer, R. and Rutkowski, D.: Multiyear trends in snowpack ion accumulation and loss, northern
911   Michigan, Water Resour. Res., 26, 721-737, 1990.

912 Swift, T. J., Perez-Losada, J., Schladow, S. G., Reuter, J. E., Jassby, A. D., and Goldman, C. R.: Water clarity
913 modeling in Lake Tahoe: Linking suspended matter characteristics to Secchi depth, Aquat. Sci., 68, 1-15,
914 2006.
915 Tarnay, L. W., Gertler, A., and Taylor, G. E.: The use of inferential models for estimating nitric acid vapor
916 deposition to semi-arid coniferous forests, Atmos. Environ., 36, 3277-3287, 2002.
917 TERC: State of the Lake Report 2011, UC Davis Tahoe Environmental Reserach Center., 2011. 2011.
918 Tranter, M., Brimblecombe, P., Davies, T. D., Vincent, C. E., Abrahams, P. W., and Blackwood, I.: The
919 composition of snowfall, snowpack and meltwater in the Scottish highlands-evidence for preferential
920 elution, Atmospheric Environment (1967), 20, 517-525, 1986.
921 Turk, J. T., Taylor, H. E., Ingersoll, G. P., Tonnessen, K. A., Clow, D. W., Mast, M. A., Campbell, D. H., and
922 Melack, J. M.: Major-ion chemistry of the Rocky Mountain snowpack, USA, Atmos. Environ., 35, 3957-
923 3966, 2001.
924 USGS: Methods for the Determination of Inorganic Substances in Water and Fluvial Sediments. U.S.
925 Government Printing Office, Washington D.C. 20402, 1985.
926 Vicars, W. C. and Sickman, J. O.: Mineral dust transport to the Sierra Nevada, California: Loading rates
927 and potential source areas, J. Geophys. Res.-Biogeosci., 116, 2011.
928 Vicars, W. C., Sickman, J. O., and Ziemann, P. J.: Atmospheric phosphorus deposition at a montane site:
929 Size distribution, effects of wildfire, and ecological implications, Atmos. Environ., 44, 2813-2821, 2010.
930 White, A. F., Bullen, T. D., Vivit, D. V., Schulz, M. S., and Clow, D. W.: The role of disseminated calcite in
931 the chemical weathering of granitoid rocks, Geochim. Cosmochim. Acta, 63, 1939-1953, 1999.
932 Williams, M. W., Bales, R. C., Brown, A. D., and Melack, J. M.: Fluxes and transformations of nitrogen in a
933 high-elevation catchment, Sierra-Nevada Biogeochemistry, 28, 1-31, 1995.
934 Williams, M. W., Brooks, P. D., Mosier, A., and Tonnessen, K. A.: Mineral nitrogen transformations in and
935 under seasonal snow in a high-elevation catchment in the Rocky Mountains, United States, Water
936 Resour. Res., 32, 3161-3171, 1996.
937 Williams, M. W., Hood, E., and Caine, N.: Role of organic nitrogen in the nitrogen cycle of a high-
938 elevation catchment, Colorado Front Range, Water Resour. Res., 37, 2569-2581, 2001.
939 Williams, M. W. and Melack, J. M.: Precipitation chemistry in and ionic loading to an alpine basin, Sierra-
940 Nevada Water Resour. Res., 27, 1563-1574, 1991a.
941 Williams, M. W. and Melack, J. M.: Solute chemistry of snowmelt and runoff in an alpine basin, Sierra-
942 Nevada Water Resour. Res., 27, 1575-1588, 1991b.
943 Zhang, Y. Y., Obrist, D., Zielinska, B., and Gertler, A.: Particulate emissions from different types of
944 biomass burning, Atmos. Environ., 72, 27-35, 2013.

945

946

7 Tables

Table 1: Analysis of variance results for 2011-12 and 2012-13 snowpack concentrations. Controlling factors of year (n=2; 2011-12, 2012-13), elevation (n=3; high, mid, low), location (n=2; east, west), and season (n=2; early, late) were investigated.

ANOVA RESULTS		TAN ($\mu g\ L^{-1}$)	NO_3^--N ($\mu g\ L^{-1}$)	Org. N ($\mu g\ L^{-1}$)	SO_4^{2-} ($\mu g\ L^{-1}$)	TP ($\mu g\ L^{-1}$)	THg ($ng\ L^{-1}$)	DHg ($ng\ L^{-1}$)
Factor:	d.f.	p-value	p-value	p-value	p-value	p-value	p-value	p-value
Year	1	< 0.01**	1	0.05**	0.26	0.27	0.1*	< 0.01**
Elevation	2	0.25	0.19	0.15	0.68	0.06*	< 0.01**	0.02**
East/West	1	0.03**	0.55	0.93	0.22	0.03**	0.23	0.46
Early/Late Season	1	< 0.01**	0.58	0.23	0.75	0.36	0.12	0.65

* p-value < 0.10

**p-value <0.05

956 **8   Figures**
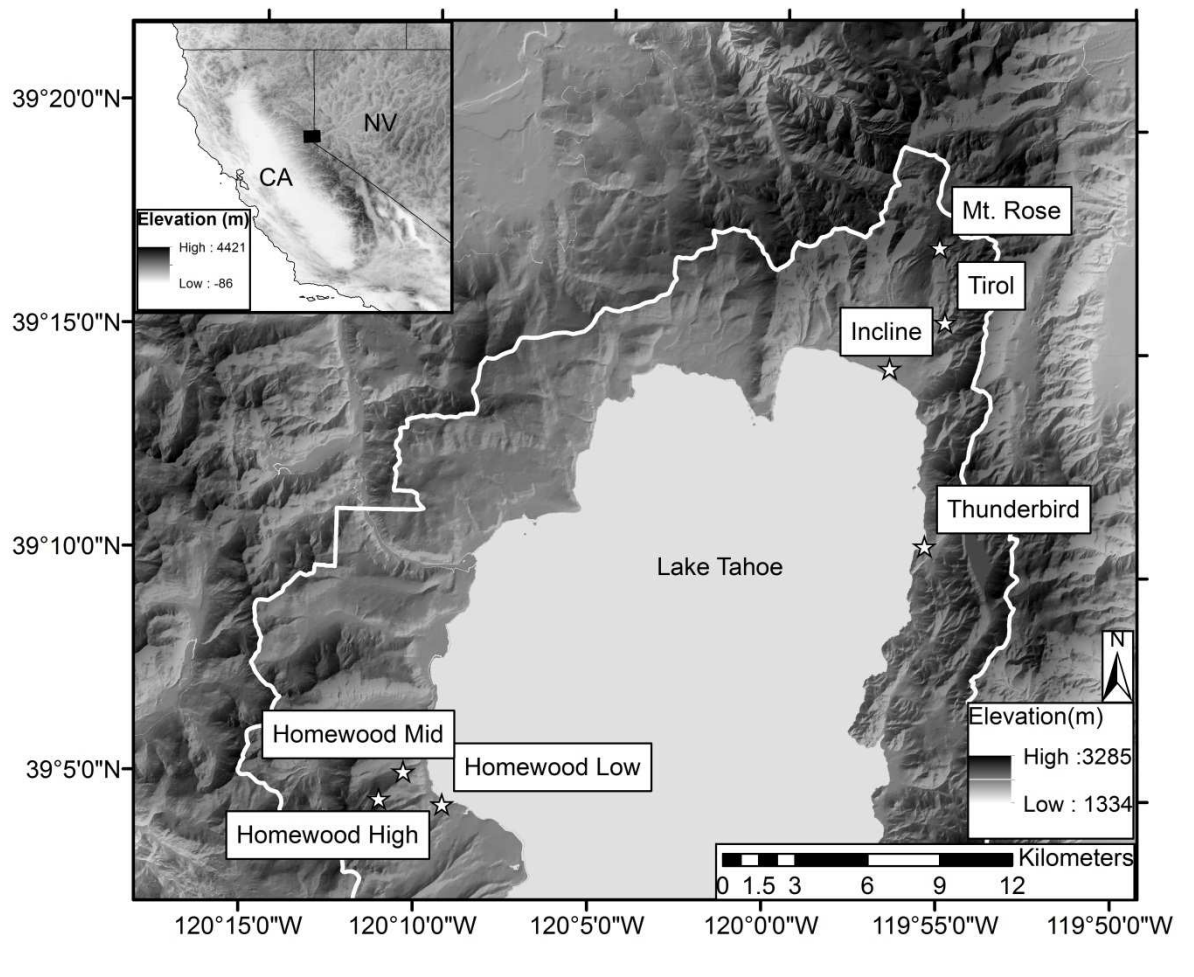
957

958   **Figure 1: Lake Tahoe watershed map with bi-weekly sampling sites located along east**
959   **and west basin elevation gradients for spatial and temporal sampling campaigns in 2011-12**
960   **and 2012-13. Additional wet deposition and snow pit profile samples were collected near**
961   **the Homewood High and Mt. Rose sites during the 2013-14 snow year.**

962

41

a) Tahoe SWE Reconstruction

WY2000-2011

b) Total N Loading

Total Loading: 113.3 (t)

c) Total P Loading

Total Loading: 9.3 (t)

d) Total Hg Loading

Total Loading: 1166.2 (g)
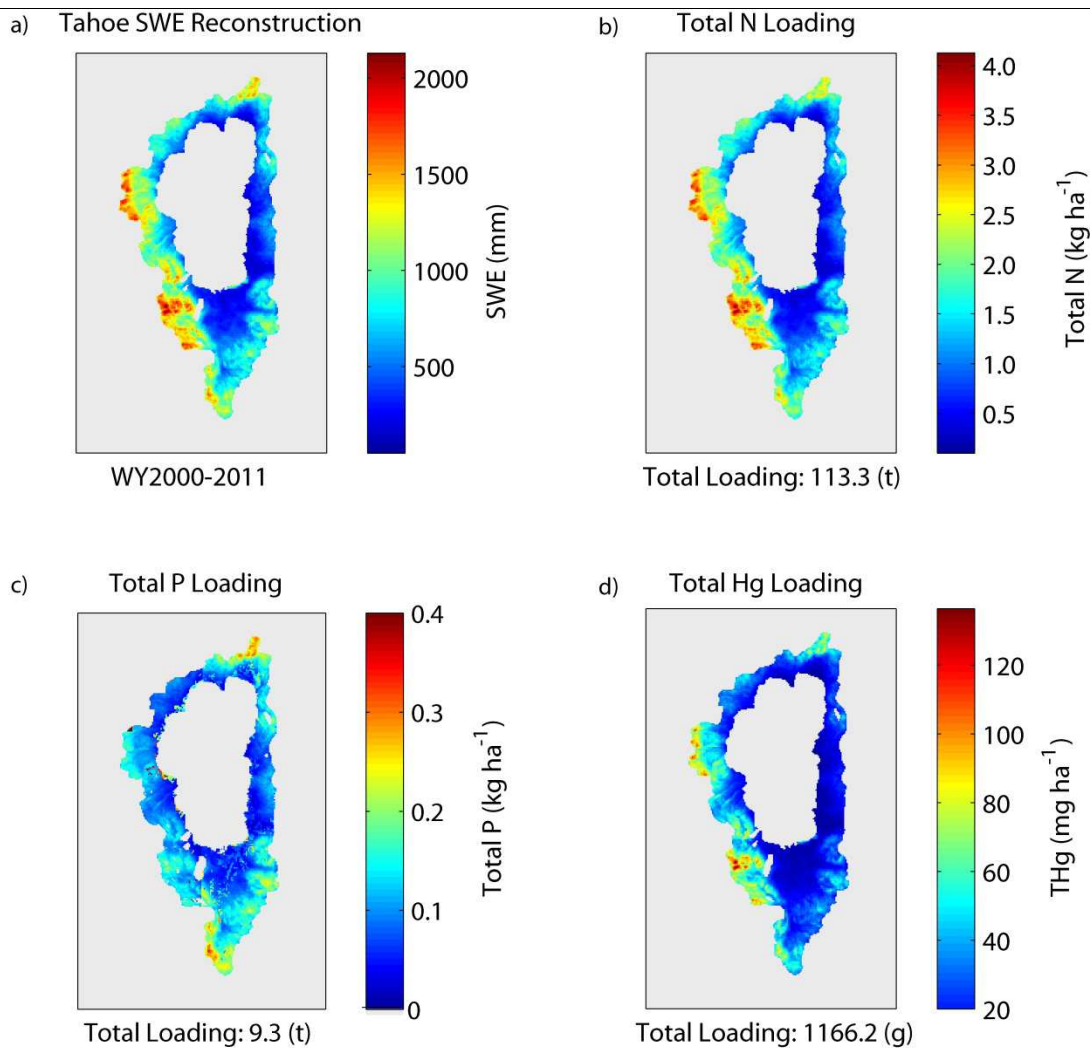
963

964 **Figure 2: (a) Decadal average (2000-2011) peak SWE for the Tahoe Basin from SWE**
965 **reconstruction for the Sierra Nevada; basin-wide peak snowpack chemical loading**
966 **estimates for (b) nitrogen, (c) total phosphorus, and (d) total Hg.**

967
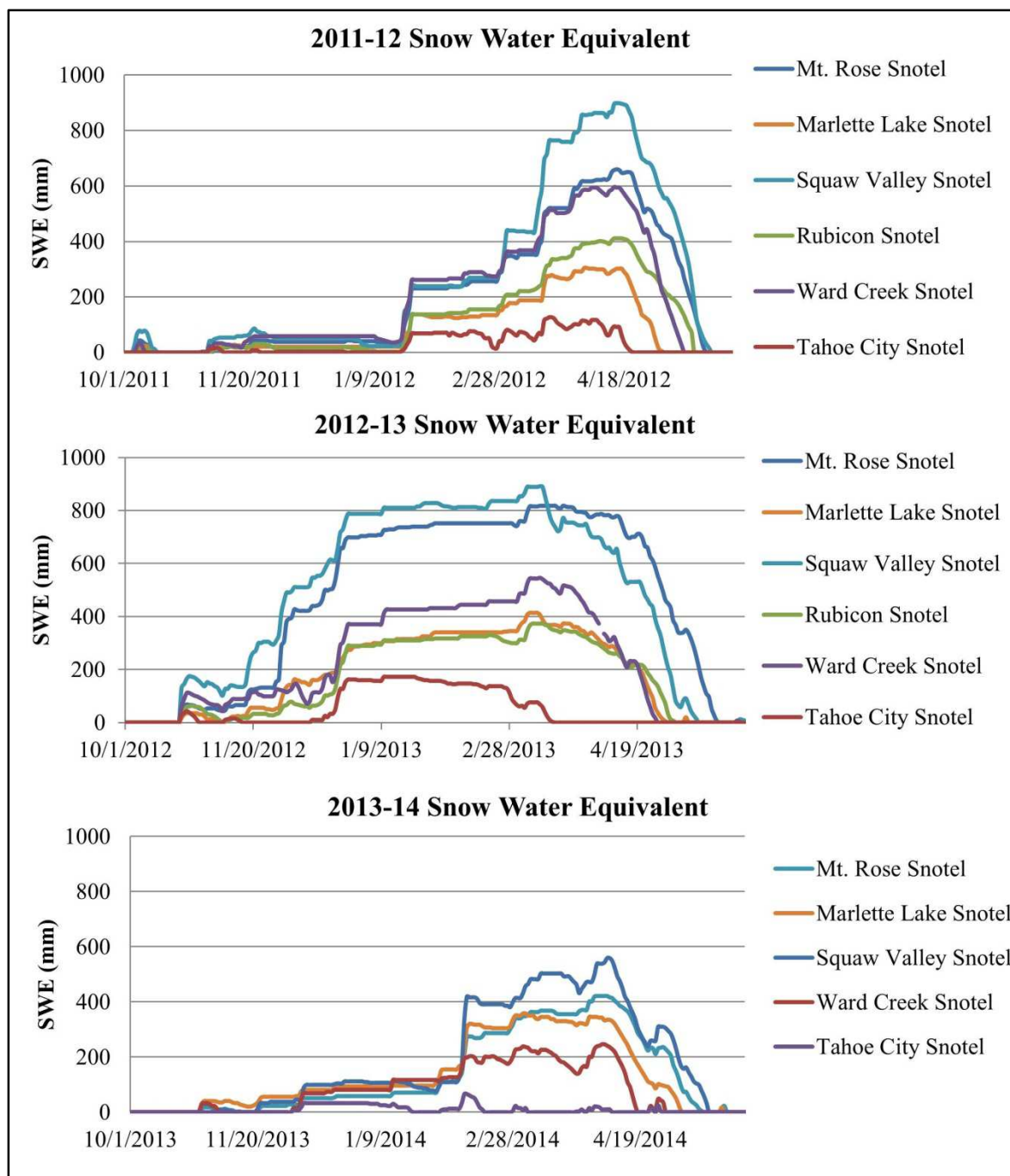
Figure 3: Snow water equivalent measured in 2011-12, 2012-13, and 2013-14 at select SNOTEL sites (NRCS, 2013) throughout the Lake Tahoe Basin.
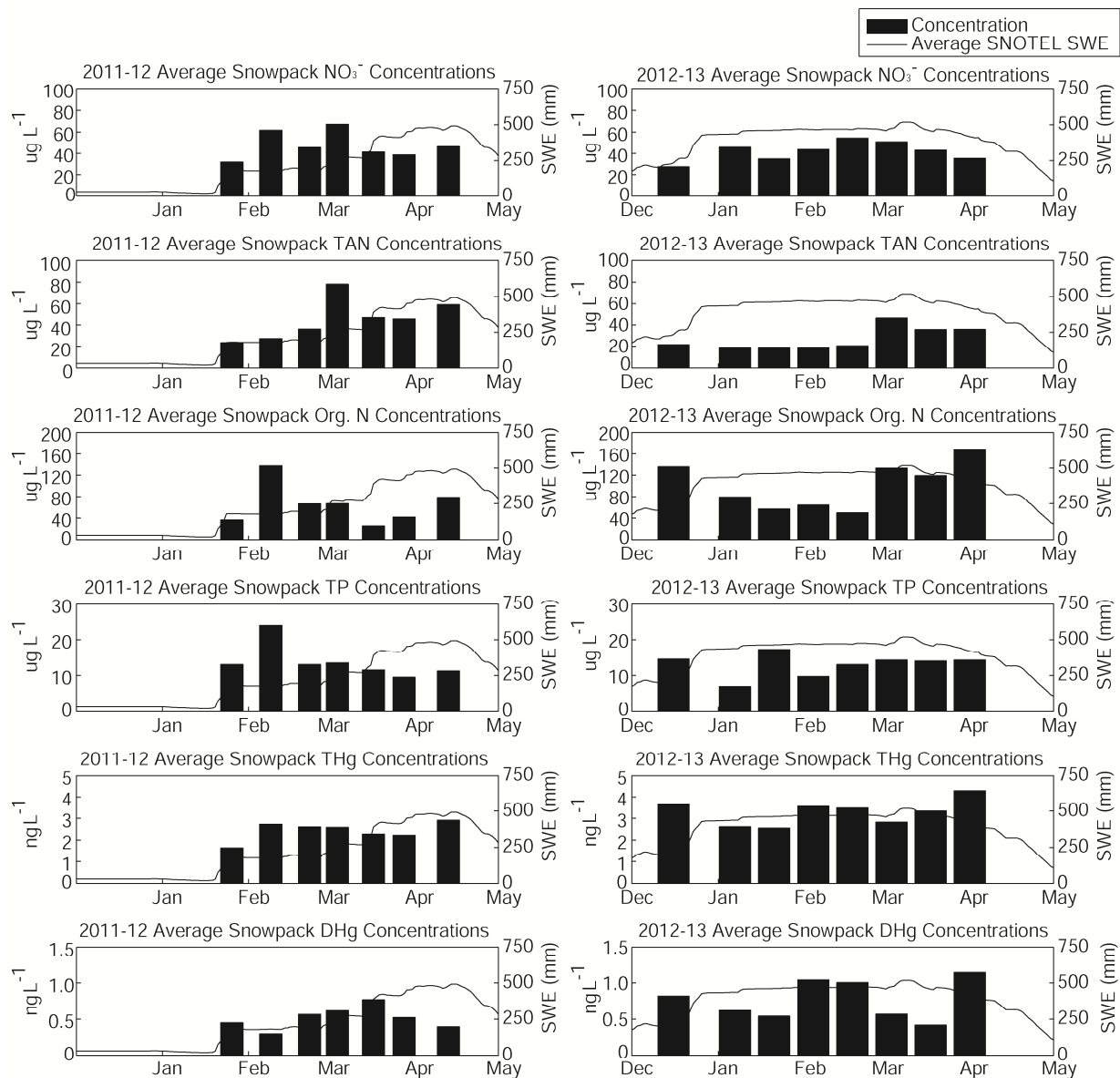
Figure 4: Average snowpack core concentrations during 2011-12 (left) and 2012-13 (right) snow seasons along with average SWE estimated from six SNOTEL sites located within the Tahoe Basin.
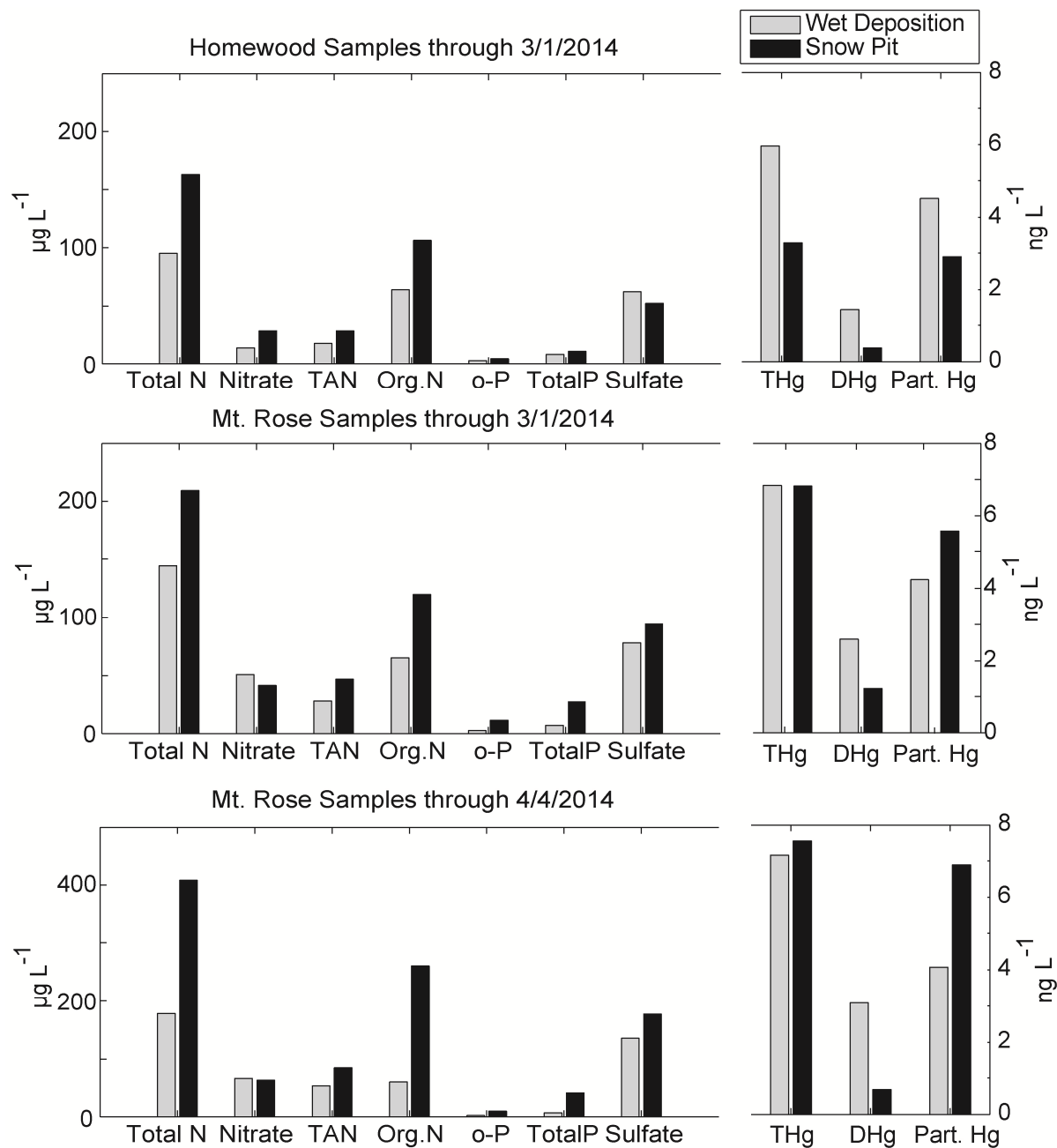
Figure 5: Comparison of seasonal average volume-weighted wet deposition concentrations with integrated snow pit samples from the 2013-14 snow year.
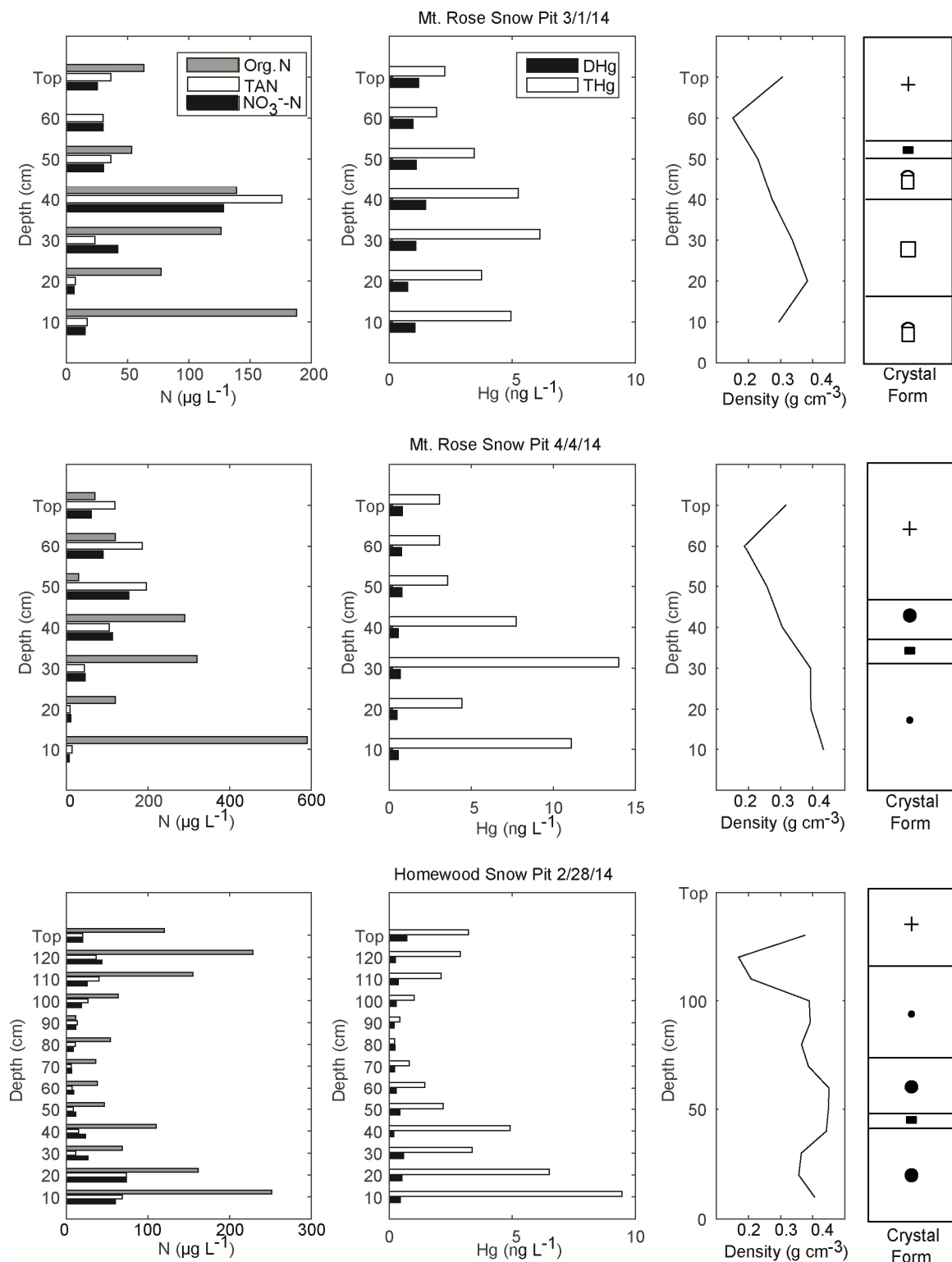
Figure 6: 2013-14 snow pit profiles for nitrogen and mercury species concentrations, snow density, and crystal form. Crystal classifications are based on the ICSI classification for seasonal snow on the ground (Fierz, 2009).

984

985

986

987

988
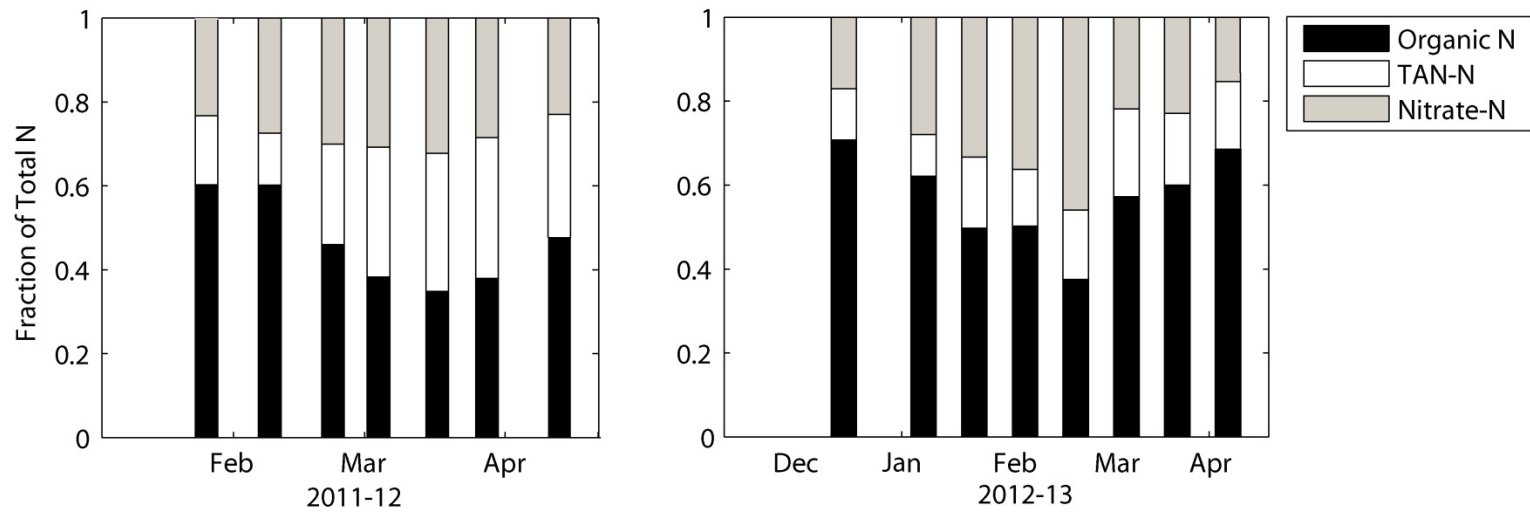
Figure 7: Snowpack total N distribution for 2011-12 (left) and 2012-13 (right).
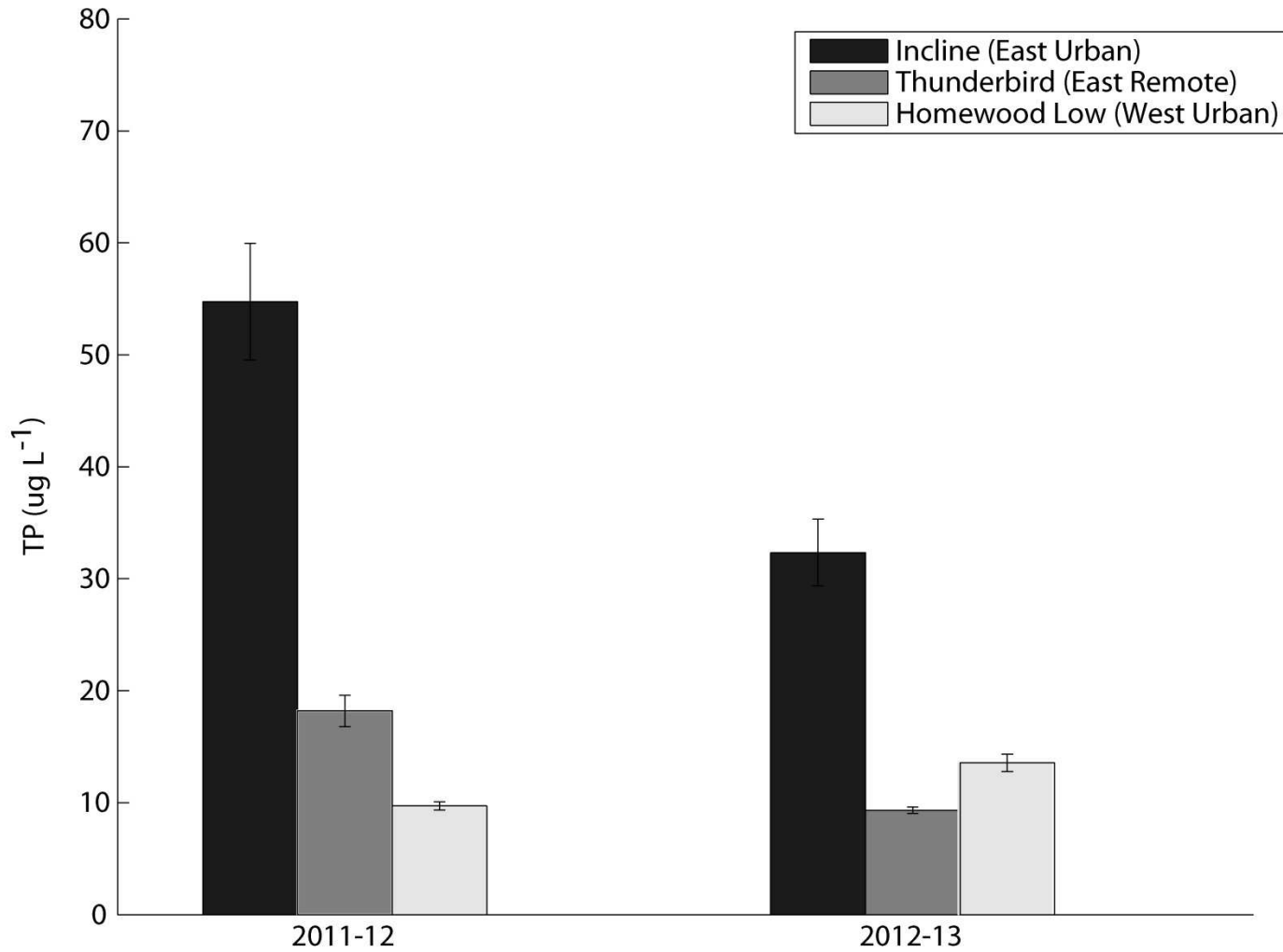
Figure 8: Average snowpack total phosphorus concentrations at all lake-level sites. The Incline and Thunderbird sites are located on the east side of the basin in urban and remote settings, respectively, and the Homewood Low site is located on the west side of the basin in an urban setting.